NASA CR-182244
RI/RD 88-273

ADVANCED SINGLE CRYSTAL FOR SSME TURBOPUMPS

by
L. G. FRITZEMEIER

ROCKWELL INTERNATIONAL
ROCKETDYNE DIVISION

prepared for
NATIONAL AERONAUTICS AND SPACE ADMINISTRATION
CLEVELAND, OHIO 44135

MARCH 1989

LEWIS RESEARCH CENTER
CONTRACT NAS3-24646
R. L. DRESHFIELD, PROGRAM MONITOR

NASA
National Aeronautics and
Space Administration

FOREWORD

The objective of this program was to evaluate the influence of commercial advanced processing methods on the mechanical properties of a single crystal nickel base superalloy. Process variables investigated were casting thermal gradient, hot isostatic pressing and alternate heat treatments.

This report describes the results of the evaluation conducted under the scope of this program.

The program was performed at the Rocketdyne Division of Rockwell International under the aegis of the National Aeronautics and Space Administration - Lewis Research Center, Cleveland, Ohio, contract number NAS3-24646. Dr. G. D. Schnittgrund of Rocketdyne Division Materials and Chemical Technology was Program Manager, Dr. L. G. Fritzemeier of Materials Engineering and Technology, was project engineer and Dr. R. L. Dreshfield was NASA Program Monitor.

TABLE OF CONTENTS

LIST OF FIGURES

EXECUTIVE SUMMARY

The primary objective of this program was to evaluate the influence of advanced processing methods on the microstructure and mechanical properties of a single crystal nickel base superalloy. A secondary purpose was to evaluate potential vendors for production of Space Shuttle Main Engine (SSME) high pressure turbopump turbine blades. The alloy chosen for the study was PWA 1480, a well characterized, commercial alloy which had previously been chosen as a candidate for the SSME high pressure turbopump turbine blades. The processing variables investigated were high thermal gradient casting, hot isostatic pressing (HIP) and alternate heat treatments. Microstructural characterization evaluated the influence of casting thermal gradient on dendrite arm spacing, casting porosity distribution and alloy homogeneity. Hot isostatic pressing was evaluated as a means of eliminating porosity as a preferred fatigue crack initiation site. The alternate heat treatment was chosen to improve hydrogen environment embrittlement resistance and for potential fatigue life improvement. Mechanical property evaluation was aimed primarily at determining improvements in low cycle and high cycle fatigue life due to the advanced processing methods. Statistically significant numbers of tests were conducted to quantitatively demonstrate life differences.

Commercial high thermal gradient casting provides a benefit in as cast homogeneity, which facilitates solution heat treatment of this turbine blade alloy. High thermal gradient casting also provides a decrease in internal pore size, which leads to increases in low cycle fatigue and high cycle fatigue life. High cycle fatigue lives are more significantly affected. Low cycle fatigue life was found to depend more strongly on yield strength than on crack initiating defects, under the conditions tested. High cycle fatigue lives are dependent both on defect size and location relative to the specimen surface. Hot isostatic pressing, when properly applied, provides dramatic increases in high cycle fatigue life, due to the elimination of casting porosity as crack initiation sites. The sensitivity of the HIP process to prior processing was demonstrated by the inability to avoid surface recrystallization due to handling damage and apparent internal recrystallization at very large pore sizes in the standard gradient material. Alternate heat treatment was found to have little influence on high cycle fatigue life in the regime tested, but affected low cycle fatigue lives by improving yield strength. Tensile properties were relatively insensitive to the HIP and high thermal gradient casting, but were somewhat improved by the alternate heat treatment. The alternate heat treatment was also shown to reduce high load, intermediate temperature, stress rupture lives.

1.0 INTRODUCTION

The most advanced, large liquid propellant rocket engine currently in service is the Space Shuttle Main Engine (SSME). This reusable engine develops 2.09 MN sea level thrust, is designed to provide 55 launches and has an operational life of 7.5 hours at rated (100%) power level. The SSME high pressure fuel turbopump (HPFTP) and high pressure oxidizer turbopump (HPOTP) are, concomitantly, the most advanced rocket engine turbines in service. Materials selection for those turbines was finalized in 1971, at which time directionally solidified, hafnium modified MAR-M246 (DS MAR-M246) (Trademark of the Martin-Marietta Company) was chosen as the turbine blade alloy. The operating environment in hydrogen fueled rocket engine turbines is significantly different from the aircraft gas turbine environment for which that alloy was developed. Rocket engine turbines operate at significantly higher rotational speeds, resulting in higher tensile, creep and fatigue mean loads, with significantly higher thermal fatigue strains and thermal shock caused by start and stop temperature transients. Rocket engine operating life limits, are, however, much shorter. As a consequence, rocket engine turbine blade materials are limited by tensile and short time creep strengths, high thermal strain low cycle fatigue, high mean stress high cycle fatigue strengths and thermal shock resistance, whereas gas turbine engine turbine blade lives tend to be limited more by long time creep strength and lower mean stress high cycle fatigue strength.

The differences in operating environment are most strongly apparent in the fundamentally dissimilar working fluids of the two classes of turbine engines. The SSME turbines are essentially high temperature steam turbines, driven by a high pressure 1:1 weight ratio of steam to unreacted hydrogen gas. The SSME is not exposed to the sulfur compounds and other by-products of the combustion processes in gas turbine engines. Foreign object damage is also highly unlikely in the closed rocket engine turbine system. Hydrogen embrittlement, however, even in the presence of water vapor, has been found to degrade many alloys.

The severe demands on the material have caused distress in the turbine blade alloy during SSME engine operation, leading to early retirement of the components. High cycle fatigue, thermally induced low cycle fatigue and hydrogen assisted cracking have all been observed at various times following post-test inspection. Recognition of this problem has led to significant effort in identification and evaluation of candidate materials for improved turbine blade capability. Single crystal superalloys were identified in an earlier study in this program as the best near-term candidate for improved SSME turbine blades.[1]

The objective of this program was to evaluate advanced processing methods as a means of further improving the properties of single crystal superalloys for rocket engine applications. Commercial high thermal gradient casting processes, hot isostatic pressing and alternate heat treatments were evaluated for potential application. Mechanical property testing was employed to quantify the expected life improvements.

2.0 PROGRAM PLAN

This program was conceived to evaluate the influence of high thermal gradient casting, hot isostatic pressing (HIP) and alternate heat treatment on the microstructure and properties of a single crystal superalloy. One objective of the program was to employ commercial processes, where possible, in order to facilitate transfer of the results to the SSME program. A secondary objective was to identify potential suppliers of single crystal turbine blades to the SSME program.

The program comprised an 36 month basic schedule, Figure 2-1, with a 6 month task included to procure additional material. Six technical tasks and one reporting task were included:

Task 1 - Literature Survey and Alloy Selection
Task 2 - Standard Thermal Gradient Solidification
Task 3 - High Thermal Gradient Solidification
Task 4 - Hot Isostatically Pressed High Thermal Gradient Castings
Task 5 - Material Evaluation
Task 6 - Additional Material (Government Deliverables)
Task 7 - Reporting

The program flow diagram is shown in Figure 2-2.

Task 1 consisted of a review of available information concerning the properties of various single crystal superalloys and selection, from the available alloys, of a candidate material to be employed in this program. Upon approval of the NASA Program Monitor, the selected alloy was cast into single crystal test bars and demonstration high pressure fuel turbopump turbine blades, employing standard thermal gradient (Task 2) and high thermal gradient (Task 3) casting processes. The distinction between standard and high thermal gradient processes was set at 30^0C/cm. Half of the material from Task 2 was heat treated according to industry practice for the alloy (standard gradient/standard heat treatment). The remaining half was hot isostatically pressed (HIP) employing a process developed by Rocketdyne prior to this program and heat treated according to an alternate schedule (standard gradient/HIP/alternate heat treatment). Half of the high gradient test material cast in Task 3 was heat treated according to the alternate heat treatment (high gradient/alternate heat treatment). The optional task, Task 4, was instituted to HIP the

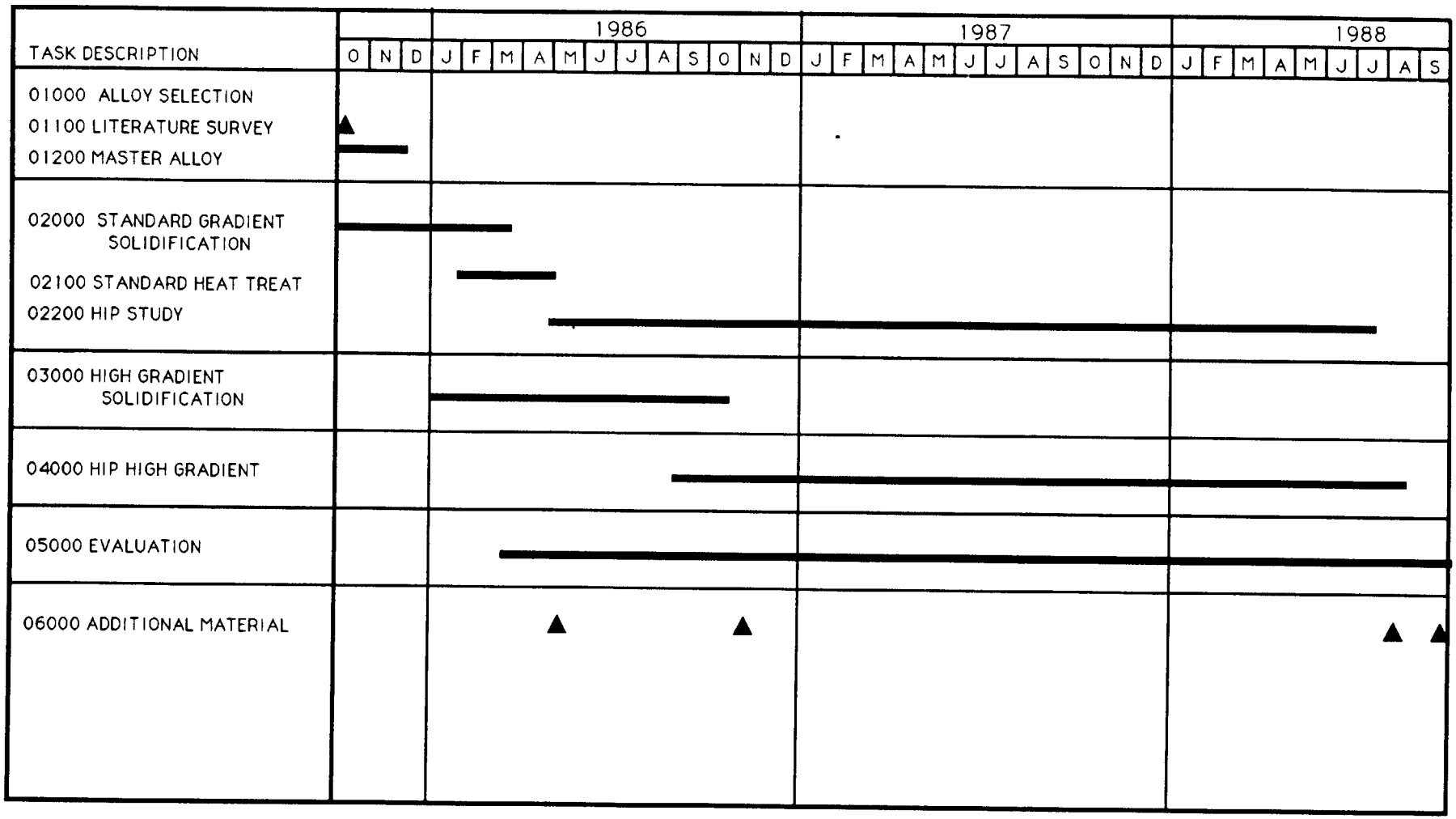

2-1 Program schedule

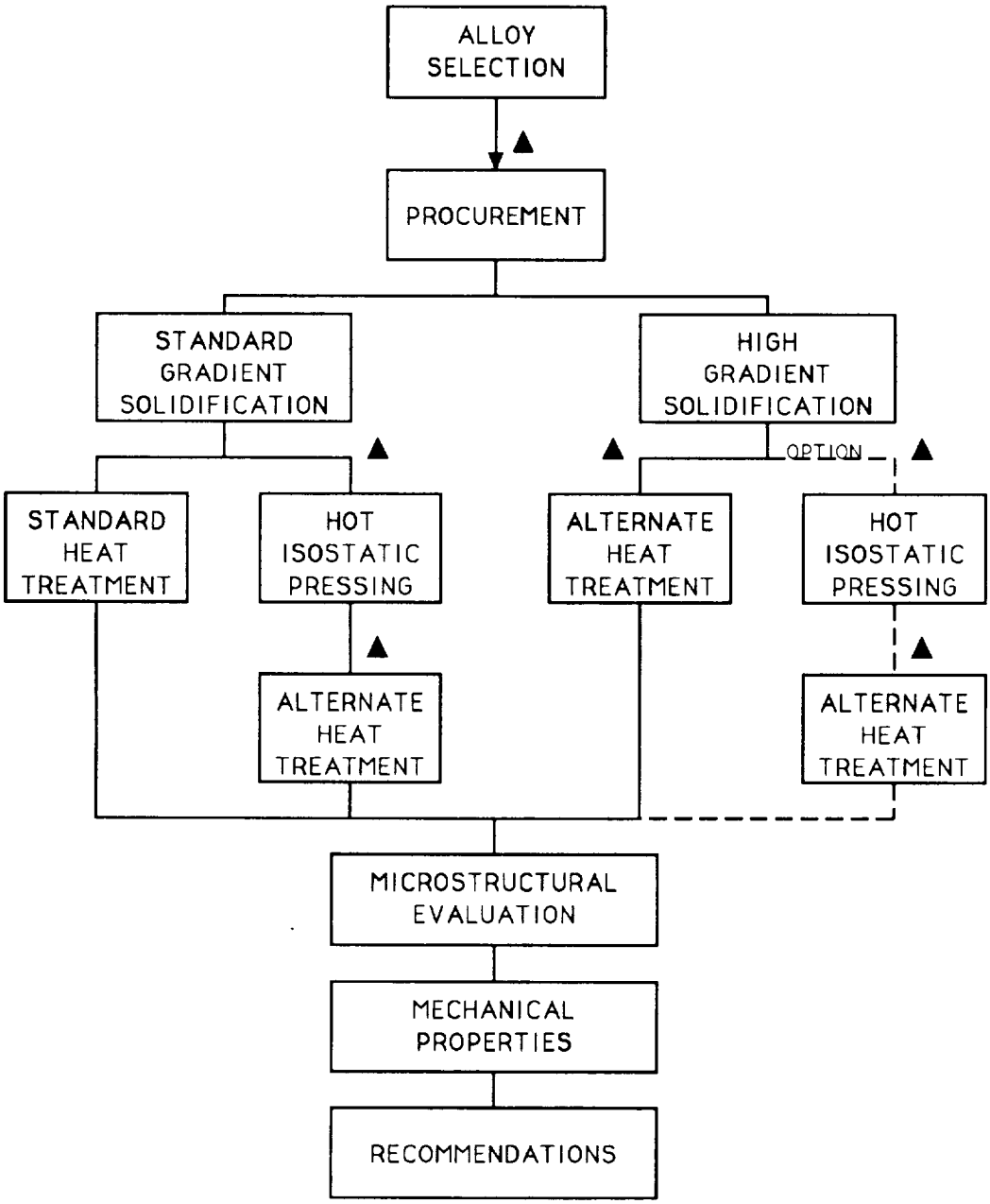

2-2 Program Flow Diagram

remaining half of the material from Task 3. This material was also given the alternate heat treatment (high gradient/HIP/alternate heat treatment). These materials were evaluated in Task 5. Metallographic evaluation was conducted to determine the influence of casting thermal gradient on homogeneity, dendrite arm spacing and porosity density and size. Scanning electron microscopy was employed to characterize the size and morphology of the strengthening γ' phase for both standard and alternate heat treatments. Mechanical testing included tensile, stress-rupture, low cycle fatigue and high cycle fatigue. Special emphasis was placed on the determination of differences in fatigue life among the material conditions. A statistically significant number of tests was conducted for each test condition. Material of each process combination was supplied to NASA-LeRC under Task 6. Both test bar castings and sample SSME turbopump turbine blade castings were supplied. Reporting for Task 7 consisted of monthly progress narratives, quarterly progress reports and oral presentations at both the NASA - Lewis Research Center and the NASA - Marshall Space Flight Center.

3.0 RESULTS

The results and discussion of the program are presented here by program task, as outlined in the preceding section.

3.1 Task 1 - Literature Review and Material Selection

Prior to selection of a single crystal superalloy for development for the SSME turbine blades, criteria were developed which the successful alloy must meet. Because of the hydrogen rich steam environment in which the blade must survive, hydrogen environment embrittlement (HEE) resistance was considered of primary importance. A candidate single crystal superalloy must exhibit HEE resistance at least equivalent to DS MAR-M246, the current SSME turbine blade alloy. Rocketdyne has developed a standard HEE screening methodology for materials to be used in high pressure hydrogen environments. Tensile tests are conducted in 34.5 MPa hydrogen environment at room temperature. Previous testing has revealed that, for most materials, hydrogen embrittlement effects are most severe at or near room temperature.[2] High pressure helium environment testing is conducted as a baseline, to minimize differences in test methodology. Both notched bar (k_t = 6.3) and smooth bar tensile tests are conducted. Embrittlement is manifested as a reduction in notched bar ultimate tensile strength, smooth bar tensile ductility or both. The ratios of the strength or ductility of the material when tested in hydrogen *versus* helium are good measures of the degree of susceptibility to HEE.

Notched bar ultimate strength ratios of the materials evaluated prior to the start of this program are shown in Figure 3-1. One of the alloys evaluated, PWA 1480, (Trademark of Pratt & Whitney Aircraft) exhibits a notched bar ultimate strength ratio superior to DS MAR-M246. Two other alloys, CMSX-2 (Trademark of Cannon-Muskegon) and Rene' N4 (Trademark of General Electric Corporation) exhibit notched bar ultimate strength ratios similar to DS MAR-M246. Only Rene' N4 and PWA 1480 also exhibit smooth bar ductility ratios clearly superior to DS MAR-M246, as shown in Figure 3-2. Of these two alloys, Rene' N4 has been replaced by a later generation alloy and is no longer commercially available. PWA 1480 is commercially available, has logged numerous flight hours in both commercial and military gas turbine engines and has undergone extensive characterization.

Only a limited amount of mechanical properties data for single crystal superalloys is available in the literature base. In general, published data focus on long term creep and

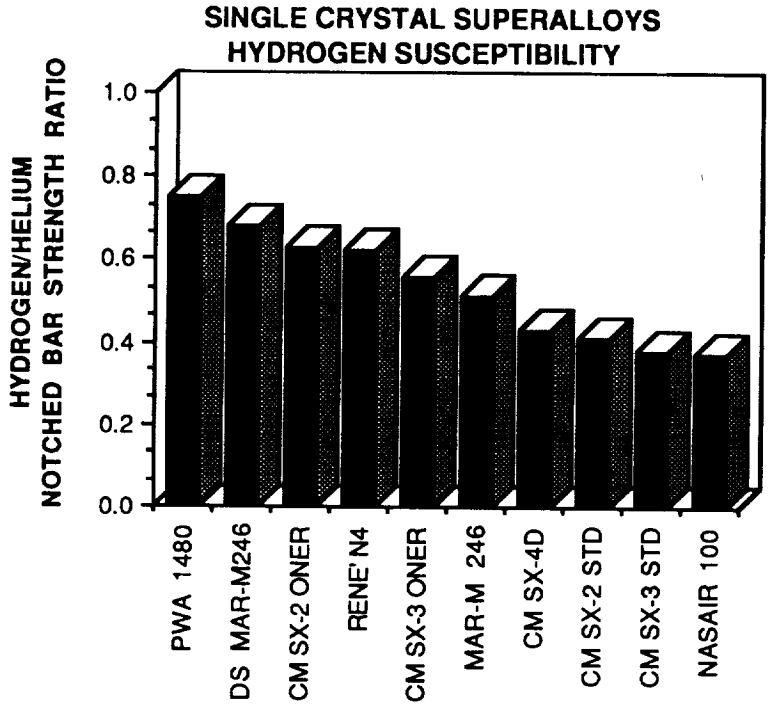

3-1 Notched bar hydrogen/helium ultimate strength ratios for candidate single crystal superalloys.

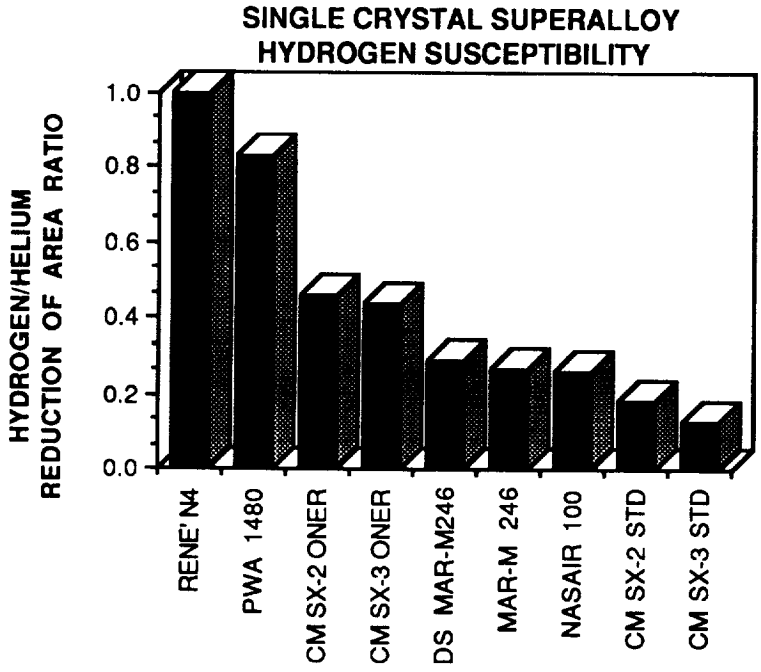

3 - 2 Smooth bar hydrogen/helium tensile ductility ratios for candidate single crystal superalloys.

3.0 RESULTS

The results and discussion of the program are presented here by program task, as outlined in the preceding section.

3.1 Task 1 - Literature Review and Material Selection

Prior to selection of a single crystal superalloy for development for the SSME turbine blades, criteria were developed which the successful alloy must meet. Because of the hydrogen rich steam environment in which the blade must survive, hydrogen environment embrittlement (HEE) resistance was considered of primary importance. A candidate single crystal superalloy must exhibit HEE resistance at least equivalent to DS MAR-M246, the current SSME turbine blade alloy. Rocketdyne has developed a standard HEE screening methodology for materials to be used in high pressure hydrogen environments. Tensile tests are conducted in 34.5 MPa hydrogen environment at room temperature. Previous testing has revealed that, for most materials, hydrogen embrittlement effects are most severe at or near room temperature.[2] High pressure helium environment testing is conducted as a baseline, to minimize differences in test methodology. Both notched bar (k_t = 6.3) and smooth bar tensile tests are conducted. Embrittlement is manifested as a reduction in notched bar ultimate tensile strength, smooth bar tensile ductility or both. The ratios of the strength or ductility of the material when tested in hydrogen *versus* helium are good measures of the degree of susceptibility to HEE.

Notched bar ultimate strength ratios of the materials evaluated prior to the start of this program are shown in Figure 3-1. One of the alloys evaluated, PWA 1480, (Trademark of Pratt & Whitney Aircraft) exhibits a notched bar ultimate strength ratio superior to DS MAR-M246. Two other alloys, CMSX-2 (Trademark of Cannon-Muskegon) and Rene' N4 (Trademark of General Electric Corporation) exhibit notched bar ultimate strength ratios similar to DS MAR-M246. Only Rene' N4 and PWA 1480 also exhibit smooth bar ductility ratios clearly superior to DS MAR-M246, as shown in Figure 3-2. Of these two alloys, Rene' N4 has been replaced by a later generation alloy and is no longer commercially available. PWA 1480 is commercially available, has logged numerous flight hours in both commercial and military gas turbine engines and has undergone extensive characterization.

Only a limited amount of mechanical properties data for single crystal superalloys is available in the literature base. In general, published data focus on long term creep and

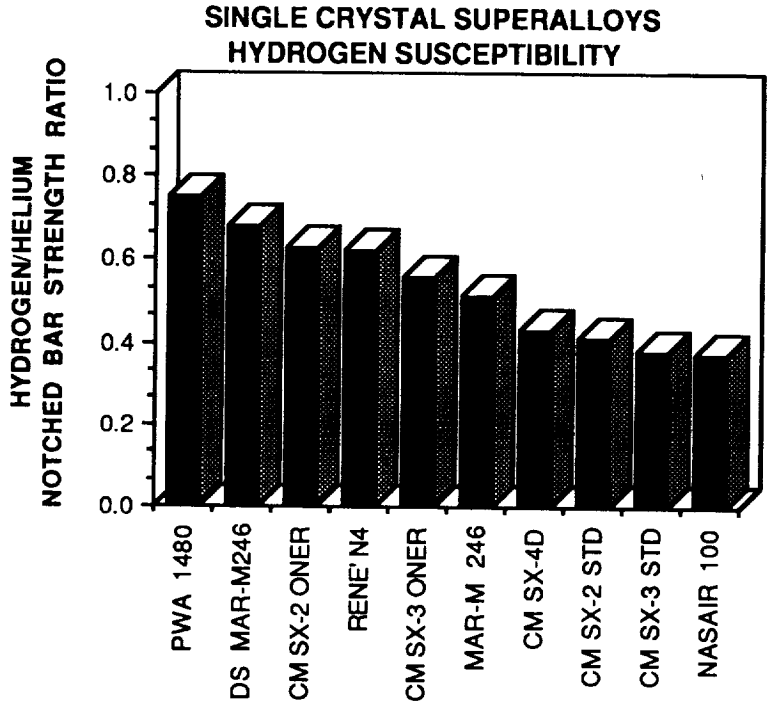

3-1 Notched bar hydrogen/helium ultimate strength ratios for candidate single crystal superalloys.

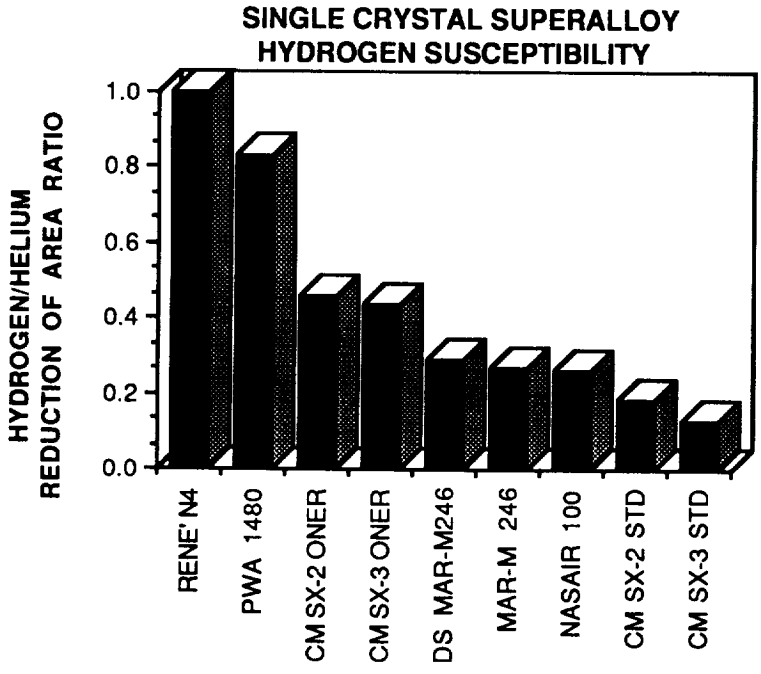

3 - 2 Smooth bar hydrogen/helium tensile ductility ratios for candidate single crystal superalloys.

stress rupture behavior and oxidation/sulfidation resistance. As discussed previously, these properties are not of primary emphasis for the rocket engine application. The published data on alloys such as PWA 1480[3], NASAIR 100[4], the CMSX series[5] and the Rolls Royce developed alloys[6] indicated that, overall, the mechanical properties of the single crystal alloys were quite similar. Rocketdyne chose PWA 1480, based upon superior HEE resistance and availability of data, as the best available alloy for the SSME applications in 1984. Rocketdyne developed an extensive data base for the production version of the alloy in the following 2 years.[7] PWA 1480 was therefore recommended, and approved by the NASA Program Monitor, as the alloy to be used in this program. Material was procured from PCC Airfoils for casting of the required single crystal samples in Task 2 and Task 3. A total of 340 kilograms of PWA 1480 master alloy meeting the requirements of Rocketdyne Specification RB0170-250 was obtained. The chemistry of the master alloy heat is given in Table 3-1.

Table 3-1 PWA 1480 CHEMISTRY
MAJOR ELEMENTS IN WEIGHT PERCENTS

	SPECIFICATION			
ELEMENT	MINIMUM		MAXIMUM	PROGRAM HEAT
NICKEL	BALANCE			BALANCE
CHROMIUM	9.5	10.5	10.16	
COBALT	4.5	5.5	5.35	
TUNGSTEN	3.75	4.25	4.13	
TANTALUM	11.75	12.25	11.95	
ALUMINUM	4.75	5.25	4.91	
TITANIUM	1.25	1.75	1.35	

3.2 Task 2 - Standard Gradient Solidification

Standard thermal gradient casting of cylindrical single crystal PWA 1480 test bars and turbine blade castings was conducted at PCC Airfoils. A number of difficulties were encountered during the course of production of the test material. It was determined that PCC had previously had some difficulty in achieving acceptable solution heat treated microstructures in PWA 1480. The microstructural specification for the program required complete solutioning of interdendritic primary γ' and no more than 2% residual casting eutectic. The solution heat treatment window, the temperature difference between the γ' solvus and incipient melting temperature, for PWA 1480 is very narrow, on the

order of 3^0C, when traditional constant temperature solution heat treatment cycles are employed. A recommended heat treatment schedule was provided for vendor evaluation and adaptation to this particular master heat chemistry. The heat treatment includes homogenizing dwell periods at temperatures approaching, and ultimately, exceeding the initial incipient melting temperature. A trial employing this heat treatment cycle was conducted. Test pieces were submitted to Rocketdyne for evaluation and the cycle was approved for solution heat treatment of the standard thermal gradient castings, based upon microstructural conformity.

The required number (20) of 1.6 cm diameter by 17.8 cm length test bars were then cast, heat treated according to the approved solution heat treatment schedule, evaluated for porosity and crystal imperfections and shipped in acceptable condition. Sixty 1.25 cm diameter by 15.2 cm length castings were poured for an expected yield of 34 pieces. The casting furnace malfunctioned during the course of the run, causing a high occurrence of grain defects in the test bars. Some of the bars exhibited acceptable primary orientations, within 10 degrees of the <001> axis, and single crystal structure. Radiographic inspection revealed detectable porosity and microstructural examination at Rocketdyne revealed the porosity level to be much higher than acceptable. New test bar castings were ordered to fulfill the program requirements and the required number of test bars was ultimately received at Rocketdyne.

It was revealed during microstructural verification, that the solution heat treatment applied to the second order of test bar castings had resulted in unacceptable incipient melting, Figure 3-3. The presence of the large amount of incipient melting was anticipated to significantly affect the mechanical properties of the baseline material and to reduce the efficiency of the HIP process. It was decided that, with the cooperation of Howmet, an experimental 'healing' heat treatment, based upon U.S. Patent No. 4,583,608, would be applied to these specimens. Some risks were associated with this decision. The increased time at the solution heat treatment temperature increases the possibility of recrystallization and grain growth from handling damage. Internal microstructure, however, was expected to be adequate since intentional incipient melting and then healing can be used to facilitate more complete solutioning without deleterious affects.[8] The resulting microstructure was acceptable according to PWA review and as confirmed by Rocketdyne microstructural analysis.

One half of the standard gradient material was heat treated according to standard practice for the alloy. The standard heat treatment consists of a two stage cycle following solution

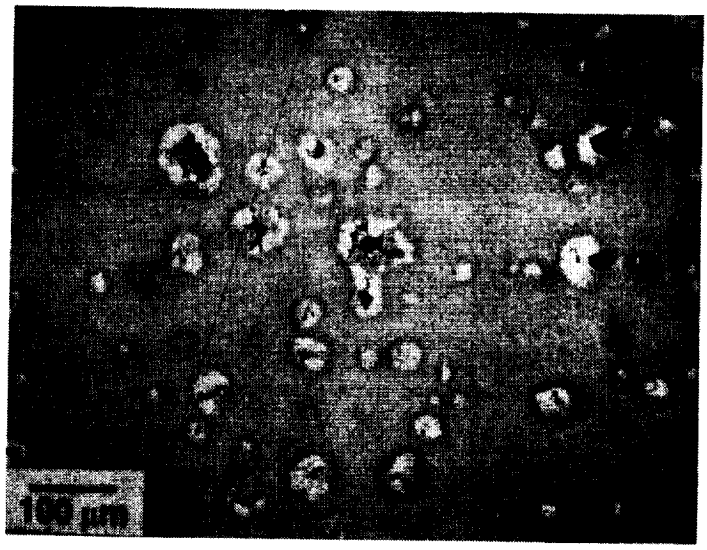

3-3 Rejectable incipient melting of standard thermal gradient castings.

heat treatment. The first stage is conducted at 1079^{0}C for 4 hours. This cycle is normally employed to diffusion bond aluminide coatings for oxidation and sulfidation protection in the gas turbine environment. The first stage also serves as the primary γ' precipitate nucleation cycle. The second stage is precipitation aging for 32 hours at 871^{0}C. This stage allows some precipitate growth and maximizes the amount of γ' in the final microstructure. The remainder of the material was HIP according to a cycle developed by Rocketdyne and later refined under the SSME program. A patent application (No. 07/033324) with notice of allowability is currently under secrecy order by the U. S. Government. The process is similar to that described in U. S. Patent No. 4,743,312. The HIP material was then submitted to a local vendor for final heat treatment. The post-HIP heat treatment cycle requires re-solution heat treatment since the cooling rate in typical HIP autoclaves is too slow to prevent gross γ' precipitation and growth. During the re-solution heat treatment, the vendor mistakenly placed the cast test pieces and demonstration turbine blade castings on a niobium sheet supported by a molybdenum hearth. The nickel-niobium eutectic temperature of 1175^{0}C is significantly below the solution heat treatment temperature of 1288^{0}C. The entire furnace load of test material, which included the high thermal gradient cast/HIP castings for Task 4, was destroyed in the subsequent meltdown. After review of possible recovery options, samples for Task 2 were substituted from Rocketdyne stock, with approval of the NASA Program Monitor. The replacement test material was procured

from the same vendor as material for this program, though at an earlier date. The chemistry of the master heat used to cast this material is compared to the original material chemistry in Table 3-2. Microstructure is considered to be equivalent to the original test material. The replacement test material was HIP and heat treated without incident. The heat treatment employed for this material employed a slightly different heat treatment cycle following solution heat treatment: 1010^{0}C for 2 hours and 871^{0}C for 48 hours. This cycle had previously been found to slightly increase the γ' size and, subsequently, improve hydrogen embrittlement resistance. Analyses of the microstructures and properties of these materials are presented under Task 5.

Table 3-2 Chemistry of PWA 1480 Substitute Material
Major Elements in Weight Percents

	Ni	Cr	Co	W	Ta	Al	Ti
Program	Bal	10.16	5.35	4.13	11.95	4.91	1.35
Replacement	Bal	10.33	5.36	4.05	11.98	4.90	1.33

3.3 Task 3 - High Gradient Solidification

The required high thermal gradient test material for this task and for Task 4 was procured from another reportedly qualified single crystal casting vendor, AE Turbine Components of Leeds, England. Test bars were cast from the master alloy procured from PCC in Task 1. A total of twenty 1.25 cm diameter by 15.2 cm long, sixty eight 1.6 cm diameter by 17.8 cm long and twelve sample HPFTP turbine blade castings were delivered. Grain defects were infrequent and the required primary crystallographic orientation of less than 10 degrees from <001> axis was met. The previously described stepped solution heat treatment was supplied to this vendor for use on the program. AETC ran an unsuccessful trial run and modified the heat treatment to account for incipient melting observed in microstructural evaluation following the trial. Subsequent trials were successful, as was the heat treatment of the deliverable items. All primary γ' was solutioned, less than 2% undissolved eutectic was present and no incipient melting was evident. Detailed analysis of the material is presented under Task 5.

3.4 Task 4 - High Thermal Gradient Cast, HIP

Test material for this task was HIP according to the previously developed cycle. Unfortunately, the original castings for this task were also included in the solution heat treatment meltdown. Replacement material for this task was also obtained from Rocketdyne

stock, with approval of the NASA Program Monitor. Castings had been previously produced by AETC, employing the same process as the material intended for this program. The replacement material was HIP and heat treated according to the alternate heat treatment cycle. Details of the microstructure and properties are presented under Task 5.

3.5 Task 5 - Evaluation

Work conducted under this task included quantitative microstructural evaluation, mechanical properties evaluation and data analysis, fractography and correlation of results.

3.5.1 Microstructural Analysis

Due to the difficulties encountered in producing and processing material for the program, the test material falls into two subsets; 1)castings originally produced for the program from the designated master heat and 2) castings produced using the same processes, but from different master heats. The use of the same casting parameters is considered to be of primary importance for this program. The master alloy chemistry differences were small and could introduce some slight differences in the results, but differences in mechanical behavior, especially fatigue, should be a stronger function of overall microstructure. Analysis of the microstructures for the different material subsets reveals that, quantitatively, the dendrite arm spacings and pore size and volume fraction are quite similar and that, qualitatively, the degree of homogeneity is similar. Small differences in alloy chemistry and the difference in time frame of the castings will be neglected for the remainder of the report.

The division between high thermal gradient casting and standard thermal gradient was set at a gradient of 30^0C/cm. Absolute measurement and comparison of thermal gradients was considered to be inaccurate due to the many variables associated with that measurement. The true solidification gradient is the temperature gradient within the solidification zone as defined by the 'mushy', or two-phase, region bounded by the melt and the fully solidified casting. The values typically measured are average gradients in the region extending into the melt. Measurement techniques are also somewhat subjective, ranging from rough measurement by thermocouples in the mold wall to rapid freezing of in-process samples and subsequent measurement of the absolute height of the two-phase region. The published typical thermal gradient for the high thermal gradient casting process employed in this effort is 40^0C/cm, well above the required cutoff limit.[9] The standard thermal gradient was known to be significantly lower, in fact, at the low end of the commercial range. The

data presented here may be considered to encompass the range expected from commercial single crystal sources.

Another casting variable influences the microstructure of directionally solidified castings. It is well known that the theoretical division between cellular and dendritic growth is represented as a constant G/V, where G is solidification gradient and V is withdrawal velocity.[10] This has been verified for the superalloys.[11] It can also be demonstrated that the fineness of the dendritic growth pattern is correlated to G x V, or solidification rate.[12] No attempt was made to control casting withdrawal rate in this program, as it was desired to utilize commercial processes. Typical casting withdrawal rates, however, are in the range of 35cm/hr.

Dendrite arm spacing measurements were made on a minimum of five metallographic sections taken from the center of representative test bars. Measurements were made on 100X photomicrographs. The number of primary dendrites was counted for each area and divided into the total area of the region to yield a dendrite 'area'. The average primary dendrite arm spacing was taken as the edge length of a square with that representative area. Typical optical photomicrographs of the cast materials are compared in Figure 3-4. The dendrite arm spacing of the standard thermal gradient casting is approximately 445 μm compared to approximately 220 μm for the high thermal gradient castings. The casting thermal gradient was calculated from the data presented by McLean,[12] shown in Figure 3-5, and assuming a withdrawal rate of 35cm/hr. The calculated thermal gradients are in reasonable agreement with the published value for the high thermal gradient casting process, as listed in Table 3-3.

Table 3-3 Calculated Casting Thermal Gradients

Casting Process	Calculated Gradient (°C/cm)	Published Gradient (°C/cm)
Standard	12	--
High	50	40

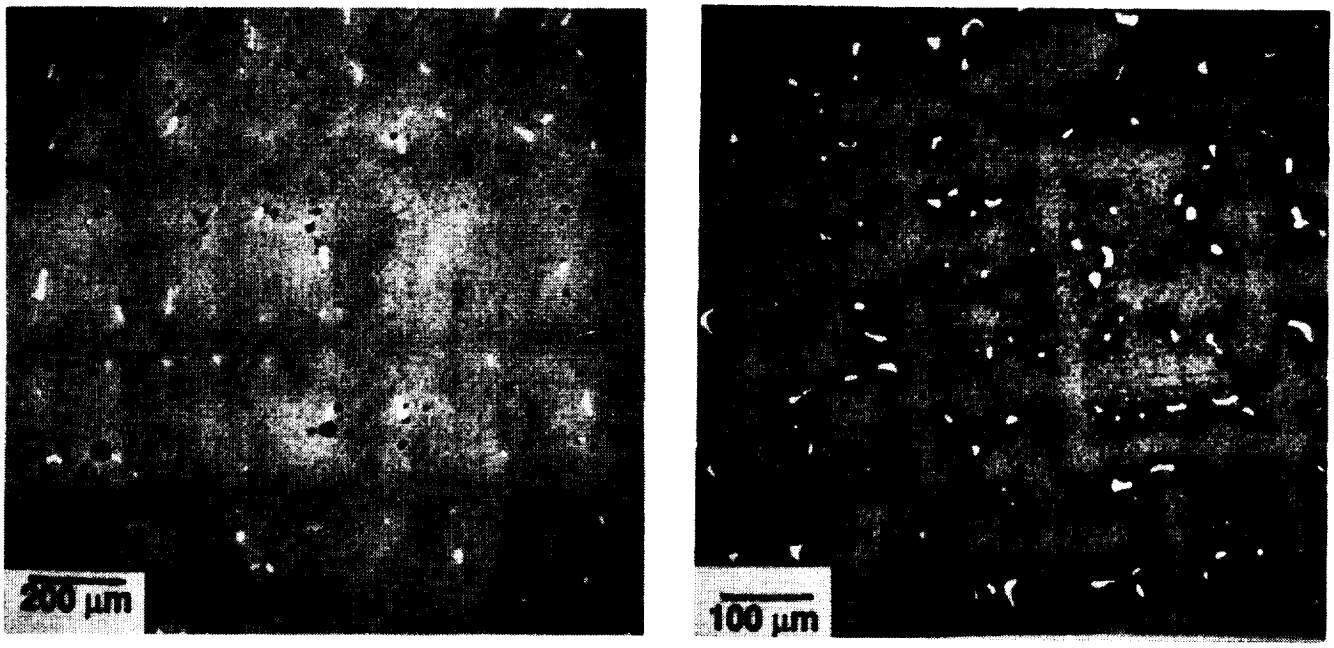

3-4 Microstructural comparison of a) standard thermal gradient and b) high thermal gradient materials.

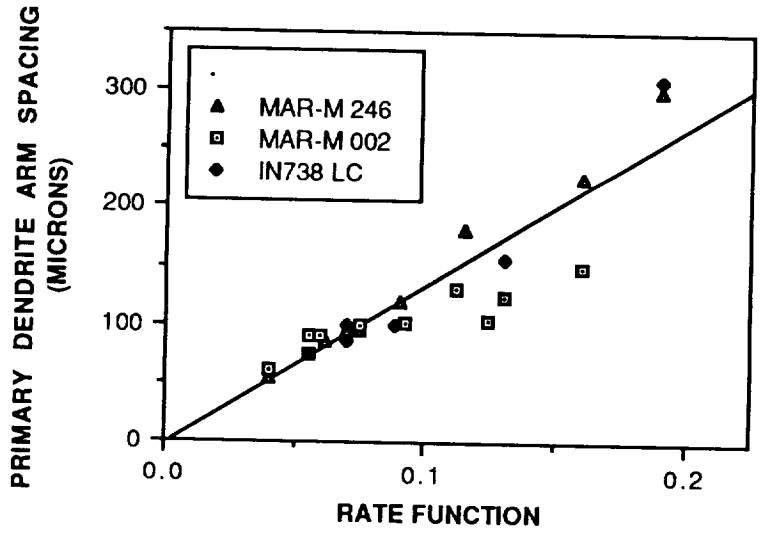

3-5 Correlation of primary dendrite arm spacing with solidification rate for three directionally solidified superalloys (from reference 12).
Rate Function = $V^{-1/4}\ G^{-1/2}$ ($m^{1/4}\ s^{1/4}\ K^{-1/2}$)

The size, distribution and area fraction of pores in the castings were also measured. Samples for porosity measurement were prepared similarly to those used for dendrite arm spacing measurements with the exception that the final polishing was conducted using only diamond slurry on silk cloth to avoid edge rounding. Samples were unetched. Typical photomicrographs of the porosity are shown in Figure 3-6. Porosity measurements were made on a quantitative metallograph. The maximum pore diameter (chord length) of each pore was measured on sections cut transverse to the crystal growth direction. The average area percent of porosity was measured for each area. Average maximum chord length, maximum observed pore size and average area percent of porosity are presented in Table 3-4. Lower bound pore sizes are dictated by the imaging system and are in the 5 μm range. The area fraction of porosity observed in the standard gradient material has been verified by independent observation.[13] Both pore size and area fraction appear to follow a

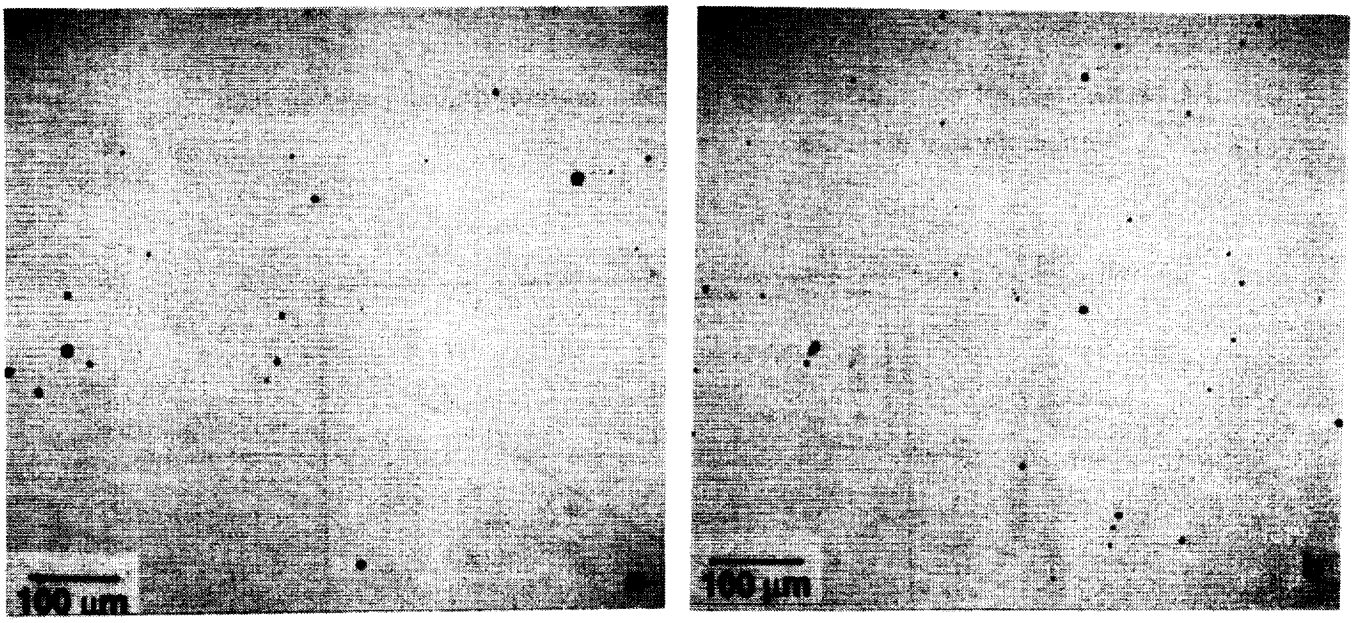

3-6 Typical casting porosity from a) standard thermal gradient and b) high thermal gradient cast PWA 1480.

correlation with dendrite arm spacing as dictated by solidification rate. The size of the metallographically observed pores, especially in the standard gradient material, was found to be much smaller than the actual pores in the material. Pores with much larger aspect ratios and larger chord lengths, even to the extent of interdendritic connection, were found on fracture surfaces and as crack initiation sites. This indicates that planar section evaluation is not sufficient to reveal the true extent of casting porosity. Larger porosity

tends to become more irregular in shape. Planar section cuts through samples are unlikely to be taken such that the true extent of the individual pores is revealed.

Table 3-4 Measured Casting Pore Sizes and Distributions

Casting Gradient	Average Pore Size (μm)	Maximum Pore Size (μm)	Area % Porosity
Standard	32	87	1.01
High	14	50	.30

As discussed previously, PWA 1480 has a limited solution heat treatment window. One benefit of high thermal gradient casting is to provide an increased degree of homogenization to the as cast structure.[14] This is qualitatively demonstrated by the ease with which the high gradient cast material was solution heat treated relative to the standard gradient castings. A peripheral advantage may be that the alloy can be HIP without danger of incipient melting and without homogenization prior to the HIP cycle. Representative photomicrographs of the fully heat treated microstructures are shown in Figure 3-7. All of the materials exhibited acceptable microstructures. The degree of solutioning improves with application of the HIP cycle and with the increased casting thermal gradient. The high gradient/HIP/alternate heat treated material exhibited 100% solutioning of casting eutectic. Small, isolated, MC-type carbides typical of this material, are visible in some areas.

Two different precipitate aging heat treatment cycles were employed following solution heat treatment of all materials. The first cycle is the standard PWA 1480 heat treatment of $1079^{0}C$ for 4 hours plus $871^{0}C$ for 32 hours. This heat treatment was applied only to the standard thermal gradient/standard heat treated material. The alternate heat treatment was originally developed under Rocketdyne internal research, for potential improvement in HEE resistance. The heat treatment was designed around the heat treatment devised by ONERA of France, for CMSX-2 and CMSX-3 alloys. Testing of that heat treatment showed a 50% improvement in hydrogen/helium ductility ratio for CMSX-2 and CMSX-3. A similar improvement was found for the alternate PWA 1480 heat treatment.[15] The goal was to provide a somewhat larger (~0.4 μm) γ' size, relative to the 0.3 μm average size in the standard heat treated condition, with a more uniform size distribution between the interdendritic and dendritic regions. A somewhat larger precipitate size is believed to reduce the planarity of slip in the alloy. This, in turn, is expected to decrease the degree of

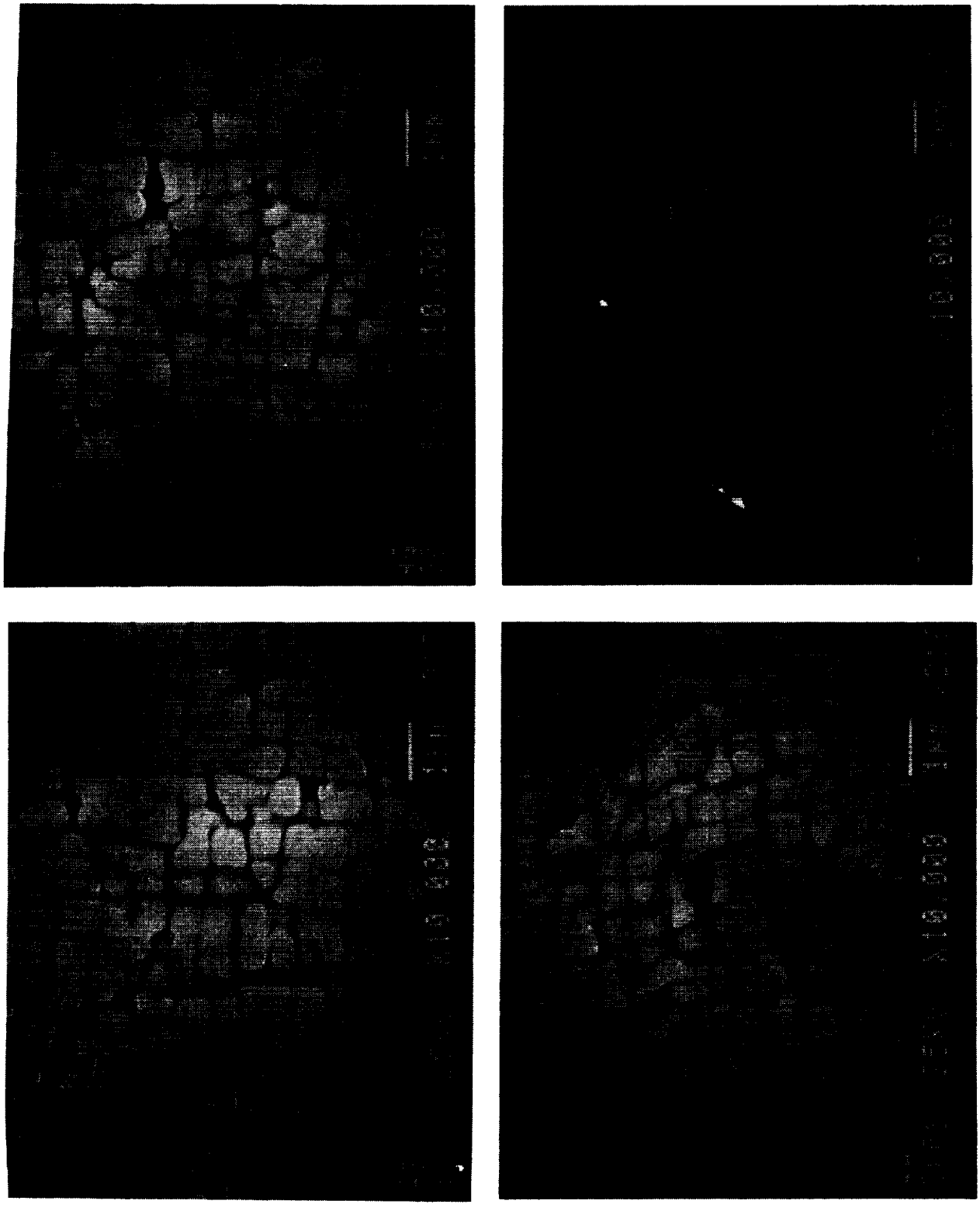

3-7 Representative heat treated microstructures for a)standard gradient/standard heat treated, b)standard gradient/HIP/alternate heat treated, c)high gradient/alternate heat treated and d)high gradient/HIP/alternate heat treated materials.

hydrogen concentration by dislocation motion and reduce the degree of HEE susceptibility. The alternate heat treatment cycle of 1010^{0}C for 2 hours plus 871^{0}C for 48 hours was applied to the standard thermal gradient/HIP material and both the high thermal gradient non-HIP and HIP materials.Scanning electron microscope photomicrographs of the γ' distributions for all of the materials are shown in Figures 3-8. In general, the desired γ' distribution is achieved with the alternate heat treatment.

3.5.2 Mechanical Properties Test Procedures

The castings and, consequently, the machined test bars employed for mechanical property evaluations were all within 10 degrees of the <001> crystallographic direction. Testing conducted prior to this program has shown that yield strength can decrease by up to 6% from 0 to 10 degrees from the <001> axis. Stress rupture lives are also slightly affected. No attempt was made to determine the precise alignment of each test sample. The slight variability in properties due to orientation is somewhat averaged by multiple tests of randomly selected samples for each test condition. Differences in properties, which fall into the expected scatterband due to orientation, are discounted as being within experimental error.

Specimens for all tests were low residual stress crush ground from the test bars produced from Tasks 2, 3 and 4. All gage sections were longitudinally polished to remove circumferential grinding marks and to further ensure low residual stress. The specimen gage diameters were 0.635 cm. Three tensile tests were conducted at room temperature (about 24^{0}C) and 760^{0}C, in air, at an engineering strain rate of 0.005/min., for each material condition. Three stress rupture tests were conducted in air at 871^{0}C, with an initial stress of 620 MPa for each material condition. Low cycle and high cycle fatigue test numbers were determined by application of "t-distribution" statistics to data for similar materials, available at the onset of the program. It was determined from that analysis that 3 low cycle fatigue tests and 8 high cycle fatigue tests for each material condition, under the same test parameters, would provide 90% confidence in a demonstrated 50% difference in life. The data generated under this program are evaluated on the same basis. The three low cycle fatigue tests were conducted in air at 538^{0}C and a fully reversed strain range of 2.0%. High cycle fatigue tests were conducted at room temperature and 871^{0}C, with an R (maximum stress/minimum stress) of 0.47. Tests were conducted at maximum stresses ranging from 793 MPa to 896 MPa, dependant on material condition. Eight tests were planned for each material condition.

3-8 Representative γ' distributions in a)standard gradient/standard heat treated, b)standard gradient/HIP/alternate heat treated, c)high gradient/alternate heat treateed and d)high gradient/HIP/alternate heat treated PWA 1480

Post-test evaluation centered on characterization of fractography and correlation of results. Details of crack initiation and propagation were catalogued.

3.5.3 Mechanical Properties Evaluation

3.5.3.1 Tensile Tests

Average tensile strengths and ductilities for the four material conditions are presented in Table 3-5. Full listings of the data are presented in the Appendix . As can be seen in Table 3-5, HIP, high gradient casting and alternate heat treatment had only a slight, if any, influence on tensile properties at room temperature but may provide an improved strength-ductility balance at 760^{0}C. Several of the standard gradient/HIP/alternate heat treated test bars failed at transverse grain boundaries. These secondary grains encompassed the entire gage section. Grains of this size are usually caused by grain growth from high residual stresses caused by surface damage incurred during handling. These test results were discounted during data analysis. The high thermal gradient/HIP/alternate heat treated material exhibits very low yield strength, especially at elevated temperature. As shown in the Appendix , the tensile properties of this material were extremely inconsistent. Only one of the three tests conducted at 760^{0}C exhibited properties consistent with the other material conditions. Review of the heat treatment records revealed that the furnace cooling rate from the post-HIP solution heat treatment temperature exceeded the 60^{0}C/minute minimum requirement. The test bars, however, were found to have been stacked in full contact in the heat treat furnace. Specific directions provided to the vendor to maintain separation between the bars were ignored. As a consequence of the close packing of the test material, the bars on the outside of the stack received adequate cooling, while those

Table 3-5 Average Tensile Test Results

Casting Gradient	Heat Treatment	Temperature (oC)	Yield Strength (MPa)	Ultimate Strength (MPa)	Reduction of Area (%)	Elongation (%)
Standard	Standard	24	1024	1075	12.5	11.7
Standard	HIP/Alt.	24	989	1219	9.2	9.8
High	Alternate	24	1080	1209	10.3	10.3
High	HIP/Alt.	24	973	1003	3.8	NA
Standard	Standard	760	1149	1273	7.6	5.0
Standard	HIP/Alt.	760	1067	1240	12.9	13.2
High	Alternate	760	1110	1303	12.6	NA
High	HIP/Alt.	760	972	1136	24.8	12.5

on the inside were cooled more slowly due to thermal mass. The properties demonstrated by the material are, therefore, biased toward the low range. Sample cutups of the test material revealed no qualitative difference in microstructure due to the slow cooling rate. Detailed analysis was not possible due to time and funding limitations.

3.5.3.2 Stress Rupture Tests

Results of the high load stress rupture tests are presented in Table 3-6. Analysis of

Table 3-6 Average Stress Rupture Results 871°C, 620 MPa Initial Stress

Casting Gradient	Heat Treatment	Time to Rupture (Hours)	Elongation (%)
Standard	Standard	14	NA
Standard	HIP/Alt.	4	22
High	Alternate	9.4	15
High	HIP/Alt.	2.8	6.2

the fracture behavior reveals that cracking initiates at internal porosity in the non-HIP material. The crack growth region surrounding the pores is in a Stage II, quasi-cleavage, mode. These cracks then link by ductile tearing of the intermediate regions. These features are indicated in Figure 3-9. A longitudinal section through the gage length of a failed stress rupture bar is given in Figure 3-10. Cracking is observed along the gage section of the bar. A higher magnification view of a pore with numerous initiated microcracks is presented in Figure 3-11.

Longer stress rupture lives of the high thermal gradient cast and/or HIP material were expected, based upon two factors. First, both processes result in a significantly greater degree of homogenization in this somewhat difficult to solution heat treat alloy. This provides a slightly increased volume fraction of strengthening γ'. The decreased alloying element segregation also allows the γ' sizes to be more closely equilibrated near an optimum size between the dendritic and interdendritic regions. A secondary factor for improved life is the reduction in size and fraction of internal casting porosity. Smaller, or eliminated, pores delay the initiation of critical size flaws until later in the creep life, thus delaying the onset of tertiary creep and ultimately, fast fracture. This effect would not be expected to be as dramatic at lower stresses and higher temperatures where aircraft operating conditions predominate. Lower (~200 MPa) applied stresses under these conditions would result in stress intensities, at the pores, below the threshold for macroscopic crack

growth. In addition, higher temperatures would promote diffuse crack tip slip processes, effectively blunting the crack and further reducing the propensity for crack growth. The observed shortened rupture lives of the advanced processed materials are believed to have been caused by the different microstructure imparted by the alternate heat treatments. A somewhat larger γ' size allows easier dislocation bypass and, hence, increases the creep rate and leads to shorter lives. This higher creep rate, apparently, more than offsets the benefits expected from reduced porosity and higher precipitate volume fraction. The extremely low life of the high gradient/HIP/alternate heat treated material is directly attributable to the relatively low strength caused by slow cooling from solution heat treatment.

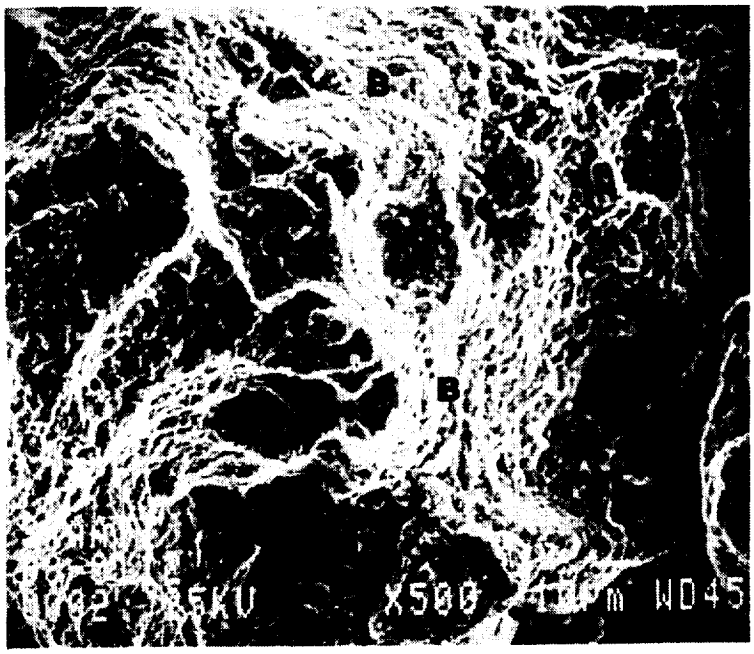

3-9 Fracture surface of a non-HIP high gradient cast stress rupture bar shows crack initiation at internal casting porosity (area A) and crack link-up by ductile tearing in intervening regions (area B).

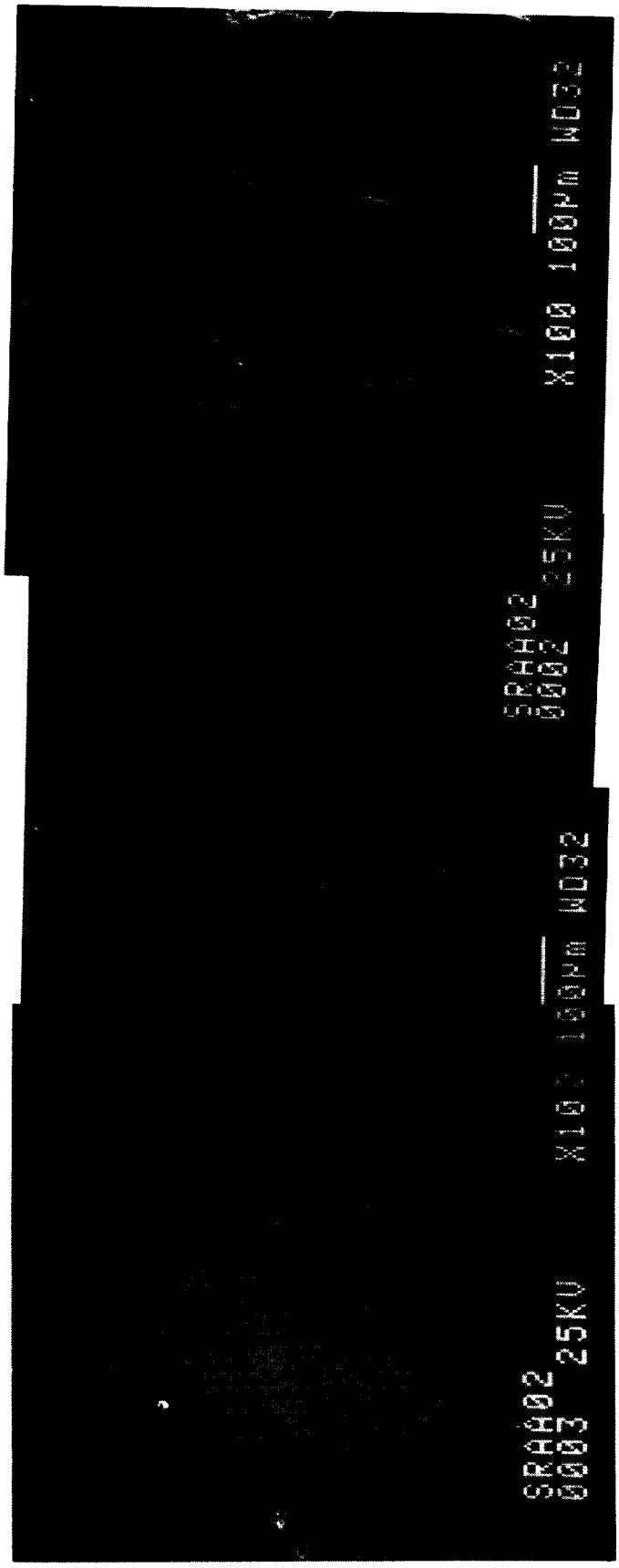

3-10 Longitudinal section through failed stress rupture sample. Fracture surface is at the right. Note crack propagation by link-up between initiation at casting porosity at arrows.

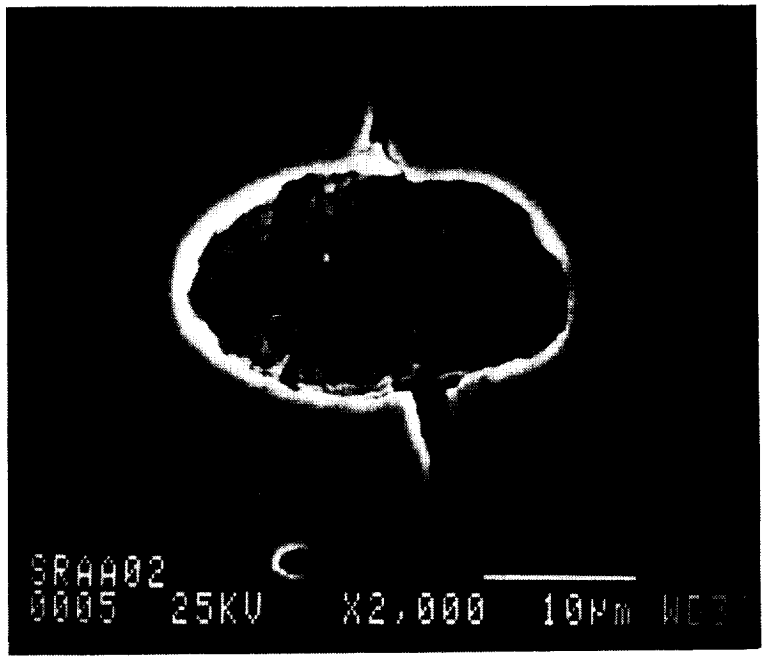

3-11 High magnification view from Figure 3-10 shows multiple crack initiation sites at casting pore.

3.5.3.3 Fatigue Tests

The *a priori* statistical analysis determined that 3 LCF tests would be adequate to demonstrate the required life differences. Low cycle fatigue test results are presented in Table 3-7.

Table 3-7 Average Low Cycle Fatigue Data
538 °C, 2.0% Total Strain Range

Casting Gradient	Heat Treatment	Number of Tests	Cycles to Failure	Standard Deviation
Standard	Standard	3	39	35
Standard	HIP/Alt.	3	78	58
High	Alternate	2	164	52
High	HIP/Alt.	3	1.5	2.2

The t-distribution calculations provide the following confidence levels for the differences in life between the indicated material conditions:

1. Standard/standard and Standard/HIP/Alternate 82%
2. Standard/standard and High/Alternate >95%
3. Standard/HIP/Alternate and High/Alternate 87%.

Comparisons between the high gradient/HIP/alternate material and the other conditions are not practical or realistic due to the poor properties associated with the slow cooling rate from the solution heat treatment. The statistics associated with the 3 other materials are very close to the 90% confidence level goal set at the beginning of the program. The comparisons clearly show that HIP and alternate heat treatment of the standard thermal gradient cast material significantly improves low cycle fatigue life. High gradient casting, even without HIP provides an additional increase over both the standard gradient/standard heat treated and the standard gradient plus HIP materials. The very low lives of the high gradient/HIP/alternate heat treated material are caused by the poor solution heat treatment, as previously discussed. The low yield strength allows a much greater amount of plastic strain for a constant applied total strain range. A plot of cyclic life as a function of

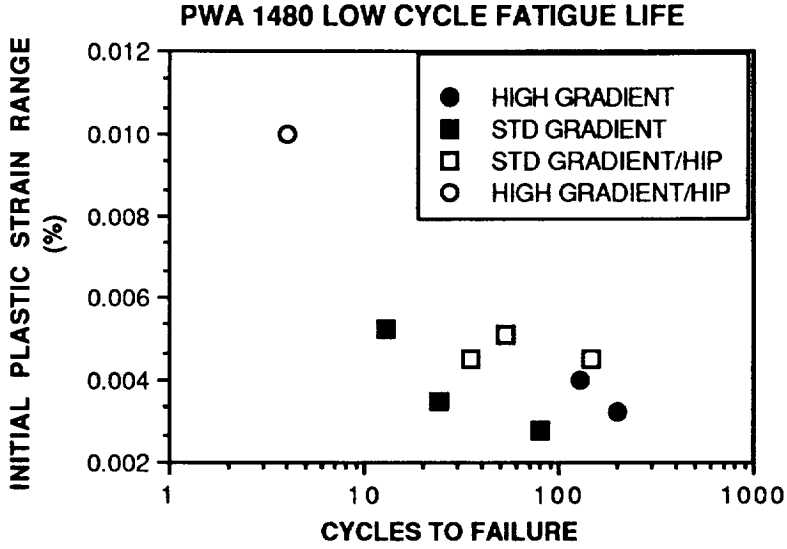

3-12 Low cycle fatigue life as a function of plastic strain range of the first full cycle.

the plastic strain range in the first full cycle is presented in Figure 3-12. Low cycle fatigue life is found to correlate roughly with plastic strain range, especially within each material condition. The peak stress in the first cycle follows an inverse relationship with plastic strain range. Although plastic strain range diminished significantly with number of cycles, very little cyclic hardening was observed in any test.

Fractographic analysis reveals that low cycle fatigue crack initiation occurs at or near the specimen surface under the conditions employed. Initiation can be traced to near surface porosity for non-HIP material and to surface associated defects such as machining marks or to slip band impingement on the specimen surface, as shown in Figures 3-13 and 3-14. Crack propagation is always Stage I, crystallographic on {111} type planes. In most cases, the fracture occurs along a single plane which encompasses the entire specimen cross section as shown in the side of a failed specimen in Figure 3-15. This fracture behavior is typical of single crystal superalloys in the low to intermediate temperature regime. The standard gradient/HIP material was found to exhibit shorter lives than the non-HIP high gradient material. It was anticipated that porosity removal would be of most benefit to the fatigue life. However, it was found that the standard gradient/HIP castings contained some

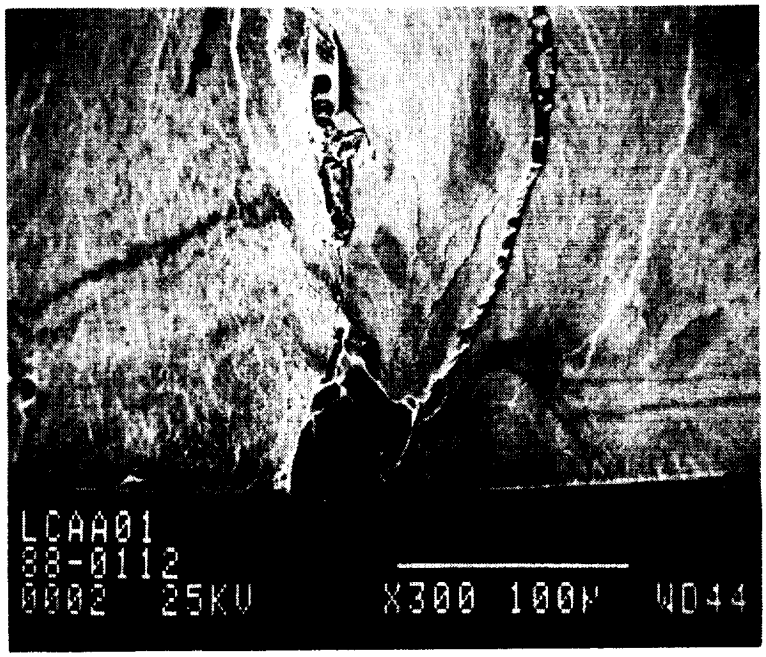

3-13 Low cycle fatigue crack initiation at near surface casting pore.

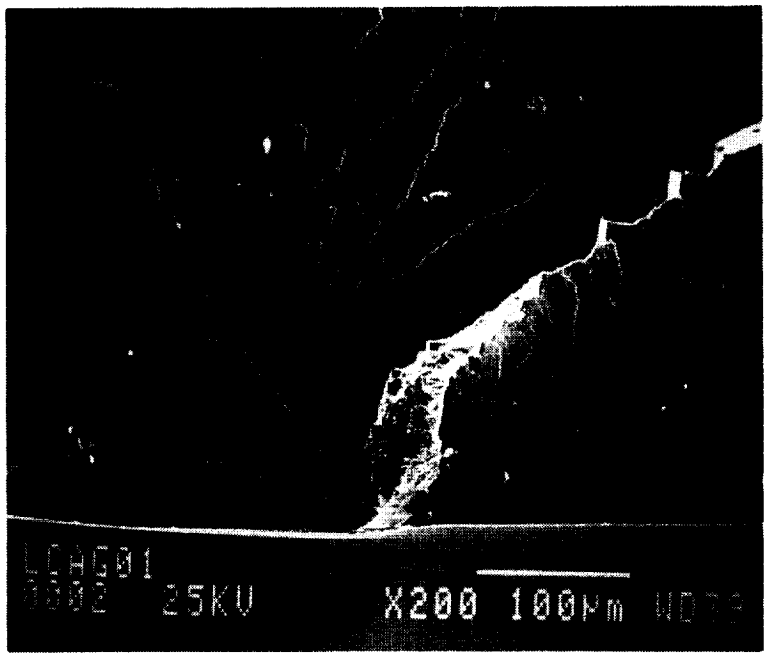

3-14 Low cycle fatigue crack initiation at specimen surface with mixed mode propagation between two intersecting {111} facets.

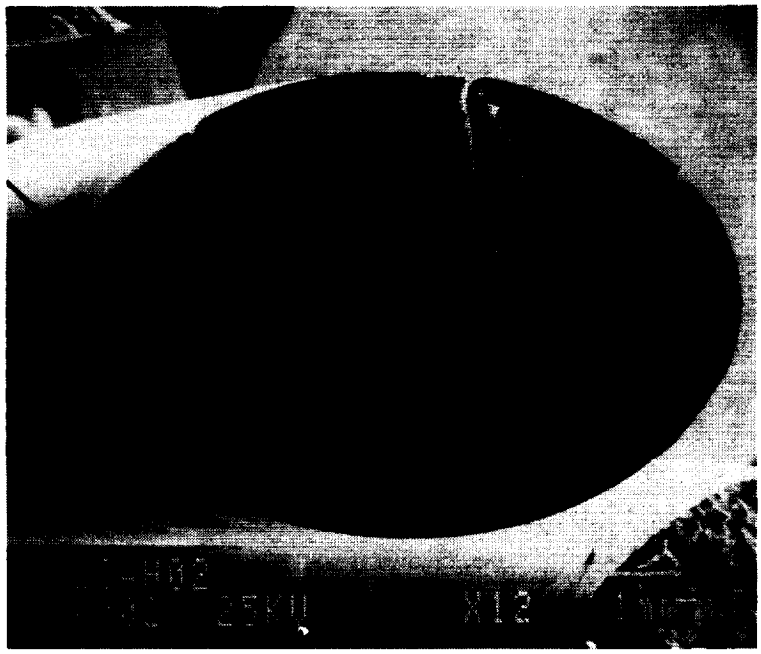

3-15 Macroscopic single facet low cycle fatigue failure. Parallel slip bands are evident on the gage length surface (arrow).

secondary grains, which may have been caused by closure of the extremely large pores occasionally found in the material.

As noted, the statistical analysis dictated that 8 samples be tested for each material condition at a given stress state in high cycle fatigue. The standard thermal gradient/standard heat treated baseline material was tested at a maximum stress of 793 MPa and a stress ratio of 0.47. Initial qualification test results for the HIP material immediately demonstrated that this maximum stress was not adequate to cause failure in less than 10 million cycles, the designated runout condition. The maximum stress was increased to cause failure in the HIP samples. Therefore, the statistical analysis cannot be directly conducted for every test condition. High cycle fatigue test results are presented fully in the Appendix . The results are discussed quantitatively and statistics are applied, where possible, in this section.

High cycle fatigue testing was the most sensitive to internal microstructure as affected by the application of advanced processing methods. A significant difference was found between the macroscopic fracture characteristics of the samples tested at room temperature versus those tested at 871^{0}C under the same stress conditions. Room temperature fractures initiated predominantly at surface, or near surface, defects. Fracture propagated in Stage I mode along intersecting {111} type planes radiating outward from the initiation site, Figure 3-16. Fractures of the samples tested at 871^{0}C generally exhibited initiation at some discontinuity in the specimen interior, though some fractures initiated at or near the specimen surface. Fractures which initiated in the specimen interior propagated in Stage II, perpendicular to the stress axis until overload occurred, Figure 3-17. The Stage II region is macroscopically very smooth. One interesting feature which was often observed was the nearly square appearance of the Stage II region. The edges of the square were found to be parallel to the <001> crystallographic directions while the diagonal was parallel to the <011> directions. Crack propagation appears to be somewhat faster in the <011> direction than in the <001> direction, an observation supported by independent crack growth measurements.[15] Fractures which initiated at or near the surface during 871^{0}C testing, initially propagated in Stage II and transitioned to mixed-mode cracking prior to overload, Figure 3-18.Some fractures of the standard gradient/HIP/alternate heat treated samples initiated at what were very clearly internal grains, Figure 3-19. The HIP cycle had not previously been shown to produce recrystallization in production quality test bars or blade castings. These grains may be either recrystallization due to HIP pore closure at the

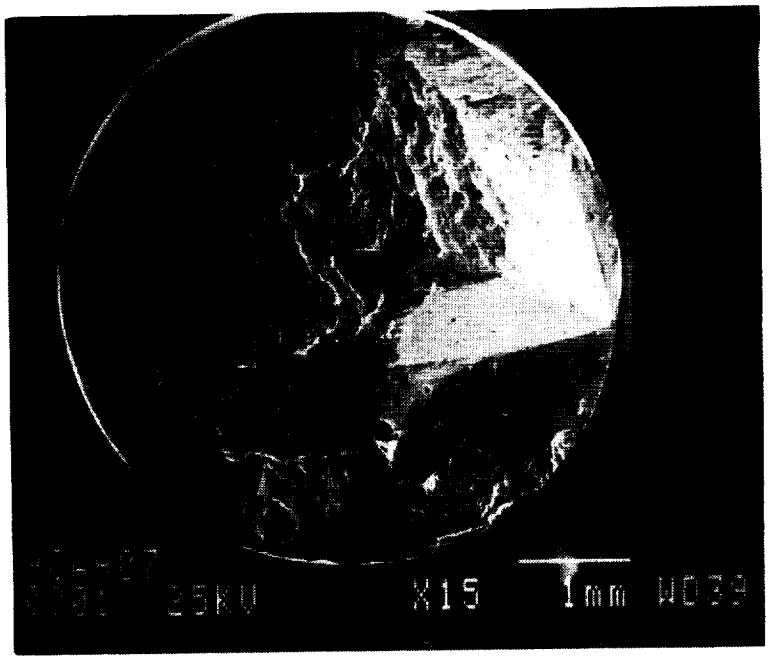

3-16 Room temperature high cycle fatigue fracture shows surface initiation and multiple facet Stage I propagation leading to overload.

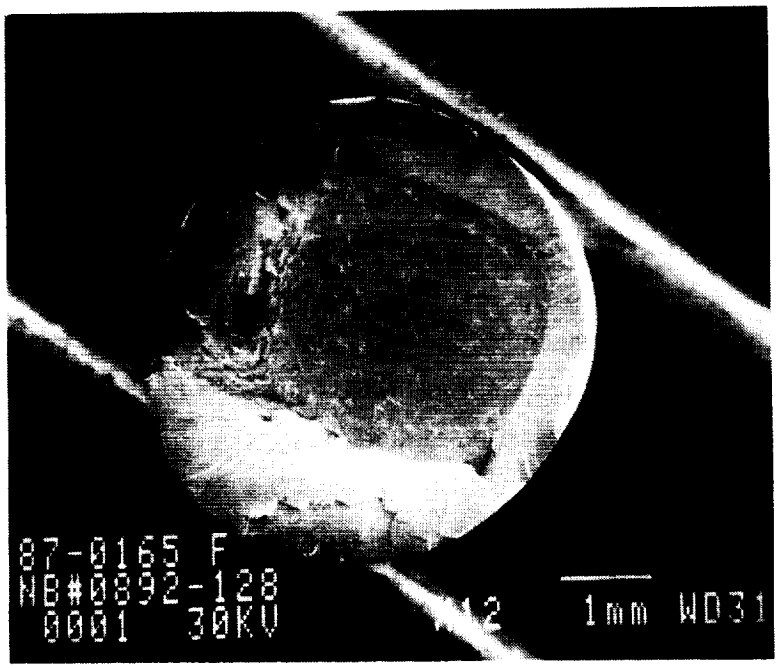

3-17 Elevated temperature high cycle fatigue fracture, initiated at internal porosity. Note rounded-square Stage II crack front.

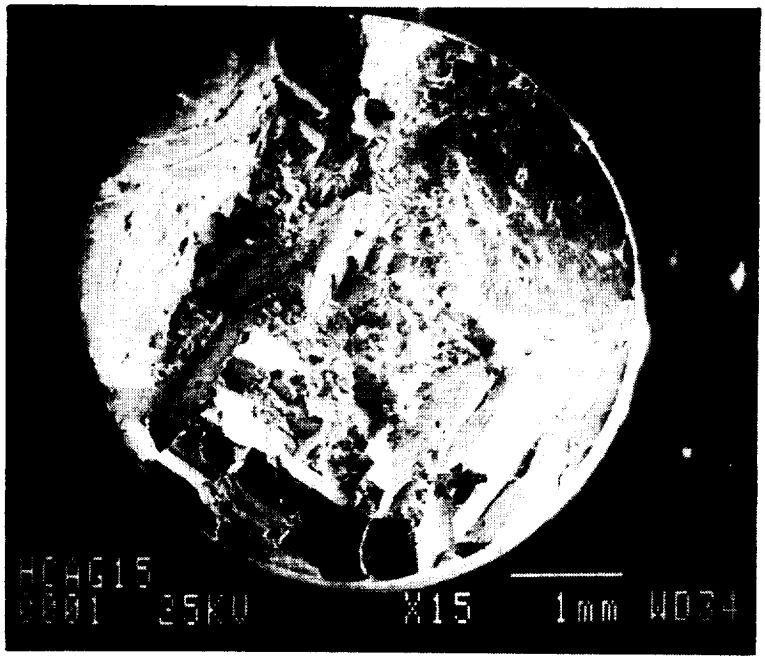

3-18 Elevated temperature high cycle fatigue fracture, initiated at surface (arrow). Propagation is Stage II followed by overload.

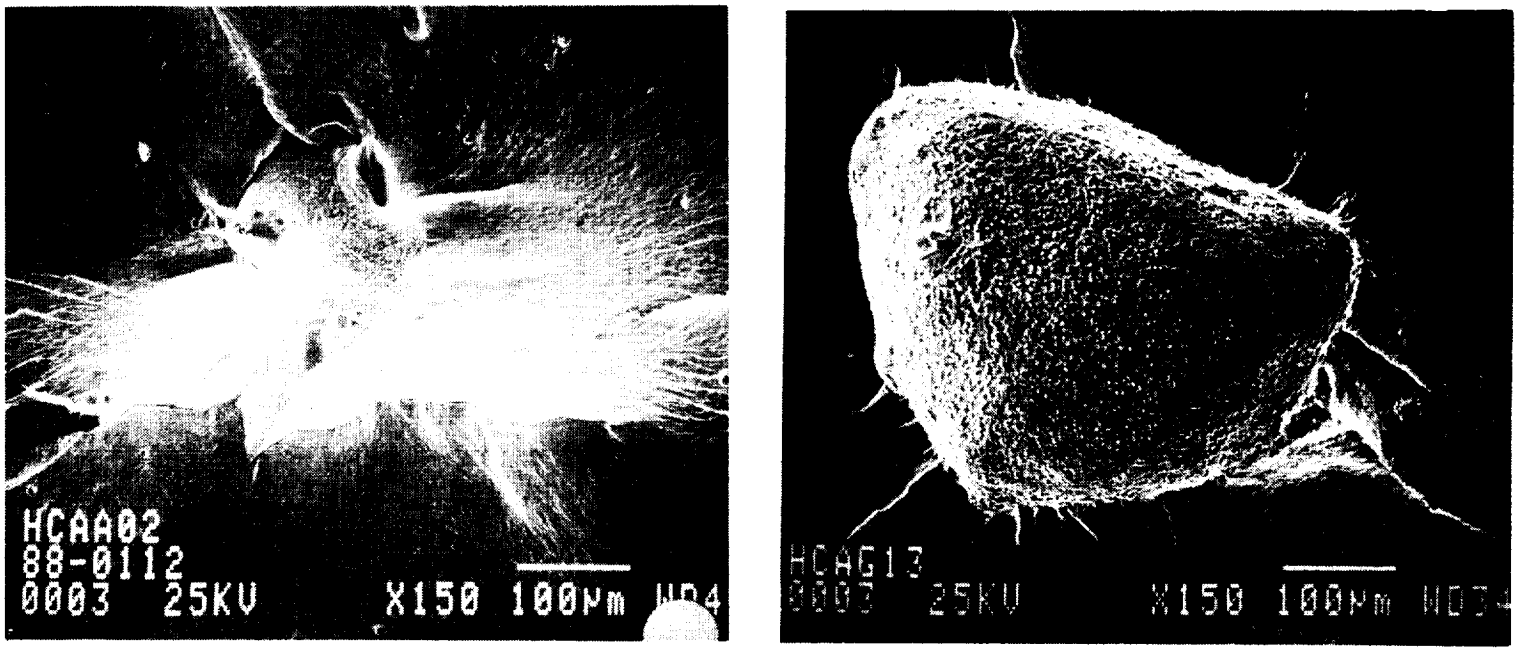

3-19 High cycle fatigue crack initiation at secondary grains in a)non-HIP and b) HIP samples.

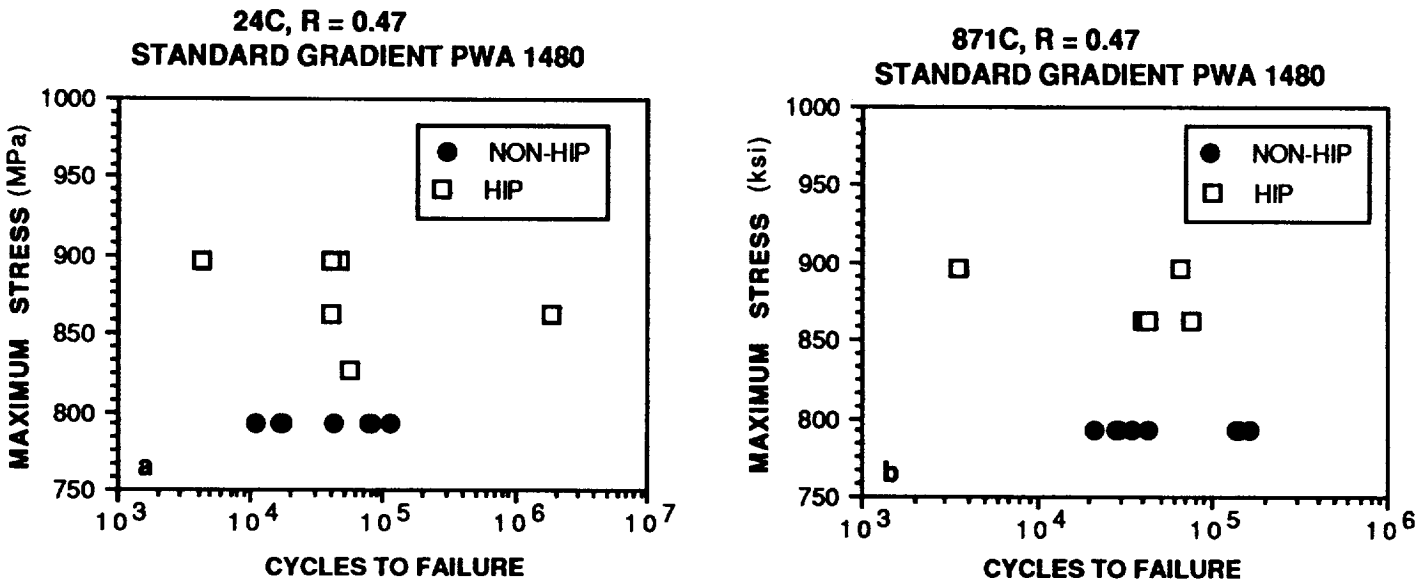

3-20 High cycle fatigue life comparison for non-HIP and HIP standard thermal gradient cast PWA 1480 at a) room temperature and b) 871C.

extremely large porosity due to the low casting gradient or secondary grains from the casting process. It should be noted that the fatigue lives of these test bars appear to exceed the lives of the standard gradient/standard heat treated alloy, Figure 3-20. Secondary internal grains, if they occur, reduce the benefit due to HIP, but some increase in life is still noted relative to non-HIP material. High cycle fatigue testing at 871^{0}C showed evidence of the poor solution heat treatment of the high thermal gradient cast/HIP/alternate heat treated material. The life of this material was statistically no different from the baseline standard gradient/standard heat treated material. This can be attributed, in part, to increased creep allowed by the large γ' precipitates.

A summary of mean life, standard deviation and number of tests conducted is presented in Table 3-8 for tests conducted at a maximum stress of 793 MPa, R=0.47 and at room temperature and 871^{0}C. Valid statistical comparison is available between the standard gradient/standard heat treated alloy and the high gradient/alternate heat treated alloy at room temperature. The t-distribution calculation reveals that the mean lives are valid with a confidence of greater than 95%. At 871^{0}C, comparison can be made between the standard gradient/standard heat treated, high gradient/alternate heat treated and high gradient/HIP/alternate heat treated materials. The difference in life between the standard gradient/standard heat treated and high gradient/alternate heat treated material is valid

with greater than 99.5% confidence.The difference between the baseline and high gradient/HIP/alternate heat treated materials is statistically negligible.

Table 3-8 High Cycle Fatigue Test Results
24°C, R=0.47,793 MPa Maximum Stress

Casting Gradient	Temperature (°C)	Heat Treatment	Number of Tests	Average Cycles to Failure	Standard Deviation
Standard	24	Standard	8	58881	42528
Standard	24	HIP/Alt.	-	- - - -	- - - -*
High	24	Alternate	4	$3.13X10^6$	$4.60X10^6$
High	24	HIP/Alt.	1	$4.30X10^6$	- - - - -
Standard	871	Standard	8	74320	60163
Standard	871	HIP/Alt.	-	- - - - -	- - - - -*
High	871	Alternate	5	$1.18X10^6$	$5.94X10^5$
High	871	HIP/Alt.	6	71246	72817

*Tested at different stress levels

3.6 Task 6 - Additional Material

A number of test bars and sample HPFTP turbine blade castings produced through each of the 4 casting and post-casting processes were required to be supplied to the NASA Program Monitor. Specifically, twenty 1.25 cm diameter by 7.6 cm long, nine 1.6 cm by 8.8 cm long test bar castings and six sample turbine blades were required for each material condition. Standard thermal gradient/standard heat treated and high thermal gradient/alternate heat treated test bar castings and sample blades were supplied from the original program material. Standard thermal gradient/HIP/alternate heat treated test material was supplied from the material substituted to replace the destroyed samples. No additional turbine blade castings were available. A new procurement of high thermal gradient test bars was needed to fulfill the contract requirement for high thermal gradient cast/HIP/alternate heat treated test material.

4.0 DISCUSSION

4.1 Alternate Heat Treatment

The influence of the alternate heat treatment on the material properties is difficult to assess. The alternate heat treatment was coupled, in every case, to another change in process variable relative to the standard gradient/standard heat treated material. The heat treatment was originally devised by Rocketdyne for potential improvements in hydrogen environment embrittlement and was employed here for possible high cycle fatigue life improvements. An addition to the program matrix, either standard gradient/alternate heat treatment or high gradient/standard heat treatment, would be required to separate the variables. Based upon the low cycle fatigue test results, an improvement in low cycle fatigue life is expected with a higher yield stress and attendant reduced plastic strain range, for a given total strain range. It is unlikely that the heat treatment would have any influence on high cycle fatigue properties. Microstructural changes, including γ' rafting, have been found to have no influence on the high cycle fatigue life of similar alloys.[16] Disregarding the interactions with HIP and high gradient casting, the current data indicate that the alternate heat treatment may improve the strength-ductility balance of PWA 1480 at elevated temperature. However, there also appears to be a detriment to high load stress rupture life at intermediate temperature.

4.2 Hot Isostatic Pressing

Hot isostatic pressing was instituted to eliminate porosity as fatigue crack initiation sites. Porosity was totally eliminated from the materials subjected to HIP in this program. The HIP cycle employed was developed to successfully HIP material produced by a casting gradient midway between the standard and high gradients used in this program. Testing of that material revealed significant improvements in low cycle and, especially, high cycle fatigue lives due to HIP. The properties of the high gradient/HIP/alternate heat treated material are poor due to the relatively low cooling rate from the post-HIP solution heat treatment. HIP of the standard thermal gradient material may have caused internal recrystallization in some of the test bars. The type of internal grains observed, however, could have been the result of secondary included grains from the casting process. Internal recrystallization could also have been caused by closure of the extremely large porosity present in this test material. This level of porosity was outside the experience range of the HIP process. Some large recrystallized grains may also have initiated at the test bar casting surface due to damage from prior handling. In addition, many of the cyclic failures were

observed to initiate at or near the specimen surface. This level of incipient melting is also beyond allowable specification limits for production quality material. Regardless of the microstructural results, the cyclic lives of this material were superior to the non-HIP standard gradient material. Even with other internal defects, the removal of the casting porosity provided improvements in fatigue lives. HIP of good quality castings with subsequent good heat treatment has been shown to provide even more life improvement.

4.3 High Thermal Gradient Casting

The primary objective of the application of high thermal gradient casting was to reduce the volume fraction and size of the interdendritic casting porosity. A significant reduction in both was observed. The primary benefit to material properties was realized as an increase in both high cycle and low cycle fatigue lives. The improvements were verified by high statistical confidence levels. Improved homogeneity, due to the high gradient casting, was not shown to have a demonstrated effect on fatigue properties. Any benefit accrued to monotonic properties as a result of high thermal gradient casting, was difficult to assess due to the introduction of the alternate heat treatment to both high gradient cast material conditions. The high gradient/alternate heat treated material did exhibit the best combination of strength and ductility at both room temperature and 760^{0}C. Stress rupture lives were found to be lowered relative to the standard material for all three advanced processed material conditions.

4.4 Interactive Effects

Interactive effects of the three advanced single crystal processing methods are difficult to assess, due in part to the coupling of the alternate heat treatment to the other techniques and due also to the difficulties encountered in the program. The benefit of high gradient casting to subsequent HIP is apparent. It may be projected that improved microstructural homogeneity can negate the need to apply a pre-HIP solution heat treatment in order to avoid incipient melting during the HIP cycle. Smaller initial pore size is also advantageous. Pore closure in high thermal gradient cast material may require less time at the solution heat treatment temperature and lower pressure during HIP. Both of these factors lessen the possibility of recrystallization due to mechanical deformation around the closing pores.

5.0 Conclusions and Recommendations

Based upon the previously discussed results, high thermal gradient casting is strongly recommended though the expected benefits are no fully demonstrated due to heat treatment problems with the HIP, high gradient material. Clear improvements to both low cycle and high cycle fatigue life were demonstrated. With the use of the standard rather than the alternate heat treatment, no adverse affects on stress rupture life should be expected. Tensile properties are also not adversely affected. The only apparent tradeoff, with improvements in high thermal gradient casting processes, is the need to adjust to production economies. Obviously, single article, laboratory scale, casting techniques cannot be feasible. The current industry trend is toward smaller furnace diameters and tailored baffling to achieve greater control over casting gradients. Exotic cooling methods, such as liquid metal cooling, are not expected to become commercial. High thermal gradient casting is helpful in providing improved homogeneity, which, in turn, may expand the useable solution heat treatment range. High gradient microstructures should also be more easily HIP by negating the need to pre-HIP solution heat treat alloys, such as PWA 1480, with narrow heat treatment temperature ranges. The high gradient material would be expected to provide wider windows for temperature and pressure during the HIP cycle.

Fatigue testing of HIP PWA 1480 under the Space Shuttle Main Engine program has demonstrated a significant increase in cyclic properties relative to non-HIP material. The data derived under this current program do not demonstrate the potential of this process. Some benefit to low cycle and high cycle fatigue lives was shown for the standard gradient/HIP/alternate heat treated material, even though that material was not of production quality. Tests results of the high gradient/HIP/alternate heat treated material were invalidated due to the poor post-HIP solution heat treatment. Because of the potential improvements due to single crystal HIP, the recommendation from this program is to further evaluate HIP single crystals, especially material produced from high thermal gradient castings.

The potential benefits due to the application of the alternate heat treat appear to be slight. High cycle fatigue lives are shown to be strongly dependent on defects and crack initiation as opposed to microstructural influences on crack propagation. Therefore, the alternate heat treatment will not influence high cycle fatigue behavior. However, the test results indicate that higher yield stress and the attendant reduction in plastic strain range, at a given total strain range, improves low cycle fatigue life. An improvement in the elevated temperature strength and ductility balance, which should improve low cycle fatigue life, was also shown.

A tradeoff with reduced stress rupture life must be considered. In general the benefits are not strong enough to warrant a significant change in processing, with the attendant need to fully recharacterize the alloy.

REFERENCES

1. W. T. Chandler, "Materials for Advanced Rocket Engine Turbopump Turbine Blades", Final Report, NASA CR-174729, November 1983.
2. R. P. Jewett, et. al., "Hydrogen-Environment Embrittlement of Metals - A NASA Technology Survey", NASA CR-2163.
3. D. P. DeLuca and B. A. Cowles, "Fatigue and Fracture of Advanced Blade Materials", AFWAL-TR-84-4167, February 1985.
4. "Materials for Advanced Turbine Engines", Final Report to NAS3-20073.
5. K. Harris, et. al., "Development of the Single Crystal Alloys CM SX-2 and CM SX-3 for Advanced Technology Turbine Blades", ASME Publication 83-GT-244.
6. D. A. Ford and R. P. Arthey, "Development of Single Crystal Alloys for Specific Engine Applications", in Superalloys 1984, M. Gell et. al., editors, pp115-124, TMS-AIME,1984.
7. Rocketdyne Materials Property Manual.
8. T. T. Field, et. al., UK Patent Application 8410036, December 1984.
9. M. J. Goulette, et. al., "Cost Effective Single Crystals", in Superalloys 1984, M. Gell, et. al., editors, pp167-176, TMS-AIME, 1984.
10. W. A. Tiller, et. al., Acta Metallurgica, 1, p428, 1953.
11. J. K. Tien and R. P. Gamble, Materials Science and Engineering, 8, pp152-160, 1971.
12. M. McLean, "Directionally Solidified Materials for High-Temperature Service", The Metals Society, London, 1983.
13. W. S. Walston, et. al., "The Effect of Hydrogen on the Deformation and Fracture of PWA 1480", in Superalloys 1988, D. N. Duhl, et. al., editors, pp295-304, 1988.
14. G. J. S. Higginbotham, Rolls Royce Ltd., personal communication.
15. Rocketdyne Division unpublished data, 1987.
16. T. S. Kahn and P. Caron, 4th RISO International Symposium on Metallurgy and Materials Science, Denmark, September 1984.

APPENDIX

Tensile Test Results

Material Condition	Specimen	Temperature (C)	Yield Strength (MPa)	Ultimate Strength (MPa)	Elongation (%)	Reduction of Area (%)
Std/Std	ABO1	20	969	969	20.0	18.3
	AB02	20	1078	1213	5.0	8.5
	AB03	20	1025	1044	10.0	10.8
	AB04	760	1169	1290	6.0	10.1
	AB05	760	1156	1258	1.0	1.6
	AB06	760	1123	1272	8.0	11.0
Std/HIP/Alt	AG01	21	983	1349	9.5	9.3
	AG02	21	971	1114	10.0	10.8
	AG03	21	1011	1194	8.0	9.4
	AG04	760	1069	1240	12.5	21.0
	AG05	760	1065	1230	14.0	16.0
	AG06	760	- - - -	691	1.0	1.6
High/Alt	AA01	20	1085	1169	10.0	10.0
	AA02	20	1087	1328	10.0	7.8
	AA03	20	1069	1128	11.0	13.0
	AA04	760	1069	1282	- -	12.4
	AA05	760	1145	1310	- -	13.1
	AA06	760	1117	1317	- -	16.3
High/HIP/Alt	AH01	21	908	952	- -	1.0
	AH02	21	985	1006	- -	1.9
	AH03	21	1027	1052	- -	8.7
	AH04	760	888	1054	- -	--
	AH05	760	896	1032	20.0	43.0
	AH06	760	1133	1322	5.0	6.7

Stress Rupture Tests at 871C

Material Condition	Specimen	Initial Stress (MPa)	Life (Hours)	Reduction of Area (%)	Elongation (%)
Std/Std	AB01	621	0.0*	- -	- -
	AB02	621	21.0	- -	- -
	AB03	621	7.1	- -	- -
Std/HIP/Alt	AG01	621	2.9	16.3	12.0
	AG02	621	0.0*	0.0	0.0
	AG03	621	5.1	35.5	33.0
High/Alt	AA01	552	63.4	14.6	- -
	AA02	621	12.7	13.8	- -
	AA03	621	6.1	16.3	- -
High/HIP/Alt	AH01	621	4.5	- -	5.9
	AH02	621	1.8	- -	6.8
	AH03	621	2.1	- -	6.2

*Failed on Load

High Cycle Fatigue Tests, R = 0.47

Material Condition	Specimen	Temperature (C)	Maximum Stress (MPa)	Cycles to Failure (x1000)	Initiation Site
Std/Std	AB01	20	793	82	Surface
	AB02	20	793	77	Surface Pore
	AB03	20	793	17	Surface Pore
	AB04	20	793	113	Surface Pore
	AB05	20	793	42	Surface Pore
	AB06	20	793	18	Surface
	AB07	20	793	11	Surface Pore
	AB08	20	793	112	Surface Pore
	AB09	871	793	159	
	AB10	871	793	137	
	AB11	871	793	29	
	AB12	871	793	42	Internal Pore
	AB13	871	793	21	Surface Pore
	AB14	871	793	143	
	AB15	871	793	35	
	AB16	871	793	28	
Std/HIP/Alt	AG01	20	862	1,900	Internal Facet
	AG02	20	896	4	Surface/grain
	AG03	20	896	45	Surface
	AG04	20	896	41	Surface

High Cycle Fatigue Tests, R = 0.47 (continued)

Material Condition	Specimen	Temperature (C)	Maximum Stress (MPa)	Cycles to Failure (x1000)	Initiation Site
	AG05	20	862	39	Surface
	AG06	20	827	56	Surface
	AG09	871	896	64	Surface
	AG10	871	896	3	Internal Grain
	AG11	871	862	41	Internal Grain
	AG12	871	862	39	Internal
	AG13	871	862	41	Internal Grain
	AG14	871	862	43	Surface
	AG15	871	862	76	Surface
	AG16	871	862	0	Failed on Load
High/Alt	AA00	871	793	925	
	AA01	871	793	997	Internal Pore
	AA02	871	793	769	Internal Grain
	AA03	20	793	957	
	AA04	20	793	190	Surface Pore
	AA05	20	793	>10,000	
	AA06	20	793	1,394	
	AA07	871	793	2,229	Internal Pore
	AA08	871	793	974	Surface Pore
High/HIP/Alt	AH01	21	793	4,300	Thread
	AH02	21	862	44	Surface
	AH03	21	862	36	Surface
	AH04	21	862	41	Surface
	AH05	21	862	33	Surface
	AH06	21	862	39	Surface
	AH07	21	862	44	Surface
	AH08	21	862	44	Surface
	AH09	871	793	171	Bad Test
	AH10	871	793	2	Thread
	AH11	871	793	86	Surface
	AH12	871	793	47	
	AH13	871	793	152	
	AH14	871	793	45	

Low Cycle Fatigue Tests at 538C

Material Condition	Specimen	Total Strain Range (%)	Plastic Strain Range First Cycle (%)	Cycles to Failure	Initiation Site
Std/Std	AB01	2.0	0.28	79	Surface Pore
	AB02	2.0	0.52	13	Plane Intersection
	AB03	2.0	0.35	24	Surface Pore
Std/HIP/Alt	AG01	2.0	0.51	54	Surface
	AG02	2.0	0.45	144	

	AG03	2.0	0.45	35	
High/Alt	AA01	2.4	0.56	32	Surface Pore
	AA02	2.0	0.40	128	Surface Pore
	AA03	2.0	0.32	201	Surface Pore
High/HIP/Alt	AH01	2.0	- -	.25	
	AH02	2.0	1.0	4	
	AH03	2.0	- -	- -	Failed on Load

NASA
National Aeronautics and Space Administration

Report Documentation Page

1. Report No.	2. Government Accession No.	3. Recipient's Catalog No.
CR-182244		

4. Title and Subtitle	5. Report Date
Advanced Single Crystal for SSME Turbopumps	March 1989
	6. Performing Organization Code

7. Author(s)	8. Performing Organization Report No.
L. G. Fritzemeier	RI/RD 88-273
	10. Work Unit No.

9. Performing Organization Name and Address	11. Contract or Grant No.
Rockwell International Rocketdyne Division 6633 Canoga Avenue Canoga Park, CA 91303	NAS3-24646
	13. Type of Report and Period Covered
12. Sponsoring Agency Name and Address	Final Contract Report
National Aeronautics and Space Administration Lewis Research Center 21000 Brookpark Road Cleveland, OH 44135-3191	14. Sponsoring Agency Code

15. Supplementary Notes

Project Manager, Dr. R. L. Dreshfield

16. Abstract

The objective of this program was to evaluate the influence of high thermal gradient casting, hot isostatic pressing (HIP) and alternate heat treatments on the microstructure and mechanical properties of a single crystal nickel base superalloy. The alloy chosen for the study was PWA 1480, a well characterized, commercial alloy which had previously been chosen as a candidate for the Space Shuttle Main Engine high pressure turbopump turbine blades. Microstructural characterization evaluated the influence of casting thermal gradient on dendrite arm spacing, casting porosity distribution and alloy homogeneity. Hot isostatic pressing was evaluated as a means of eliminating porosity as a preferred fatigue crack initiation site. The alternate heat treatment was chosen to improve hydrogen environment embrittlement resistance and for potential fatigue life improvement. Mechanical property evaluation was aimed primarily at determining improvements in low cycle and high cycle fatigue life due to the advanced processing methods. Statistically significant numbers of tests were conducted to quantitatively demonstrate life differences.

High thermal gradient casting improves as-cast homogeneity, which facilitates solution heat treatment of PWA 1480 and provides a decrease in internal pore size, leading to increases in low cycle and high cycle fatigue lives. Low cycle fatigue life was found to depend more strongly on yield strength than on crack initiating defects. Elimination of casting porosity by hot isostatic pressing can provide dramatic increases in high cycle fatigue life. Alternate heat treatment had little influence on high cycle fatigue life but affected low cycle fatigue lives by improving yield strength. Tensile properties were insensitive to HIP and high thermal gradient casting, but were somewhat improved by the alternate heat treatment which also reduced high load, intermediate temperature, stress rupture lives.

17. Key Words (Suggested by Author(s))		18. Distribution Statement
Superalloys	Single Crystal	Unclassified - Unlimited
Hot Isostatic Pressing	High Gradient Casting	Subject Category 26
Alternate Heat Treatment	Space Shuttle Main Engine	
Low Cycle Fatigue	High Cycle Fatigue	

19. Security Classif. (of this report)	20. Security Classif. (of this page)	21. No. of pages	22. Price
Unclassified	Unclassified	48	A03

NASA FORM 1626 OCT 86